Accompanying material from the thesis entitled “Initiation of Nuclear DNA Replication in *Trypanosoma brucei* and *Leishmania*”, submitted by Catarina de Almeida Marques in fulfilment of the requirements for the Degree of Doctor in Philosophy.

Wellcome Trust Centre for Molecular Parasitology; Institute of Infections, Immunity and Inflammation; College of Medical, Veterinary and Life Sciences

University of Glasgow

April 2015

Table of Contents

List of Tables

List of Figures

7 Appendices

7.1 Conservation of the putative origin recognition complex factors within the kinetoplastid group

Figure 7.1. The putative ORC factors are syntenic between different kinetoplastid species. Each panel (A-F) represents a 10 Kbp window of the parasite's genome (top row shows the *T. brucei* chromosome as well as the chromosome coordinates). The *T. brucei* (Tb927) gene of interest is highlighted in yellow, and the respective orthologues in *L. major* (Lmaj), *L. mexicana* (Lmex) and *T. cruzi* (TcNEL) are shown in the "syntenic sequences and genes" section. A) shows the orthologues of TbORC1/CDC6; B) orthologues of TbORC1B; C) orthologues of TbORC4; D) orthologues of Tb7980; E) orthologues of Tb3120; and F) orthologues of Tb1120. Images retrieved from TriTrypDB version 8.0. *(continued below)*

D)

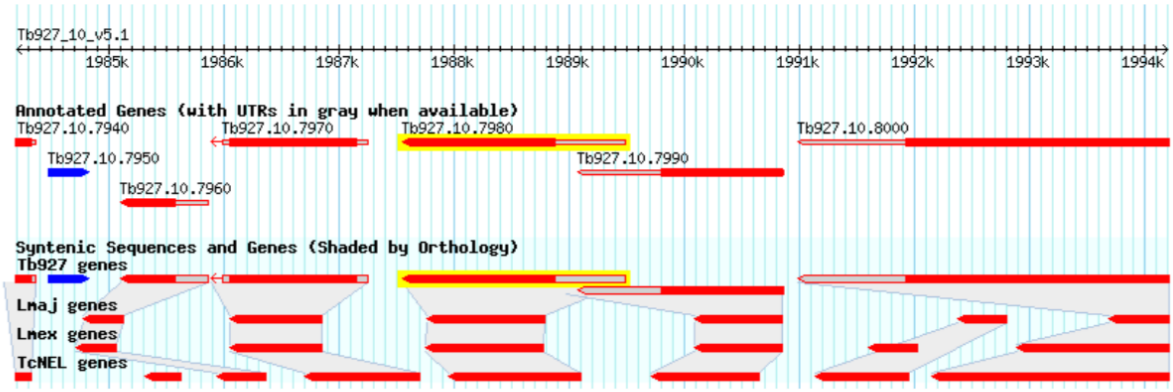

E)

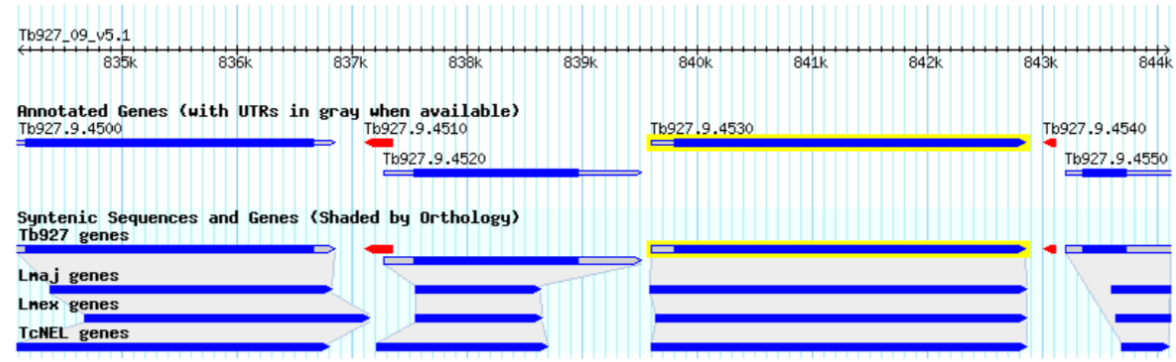

F)

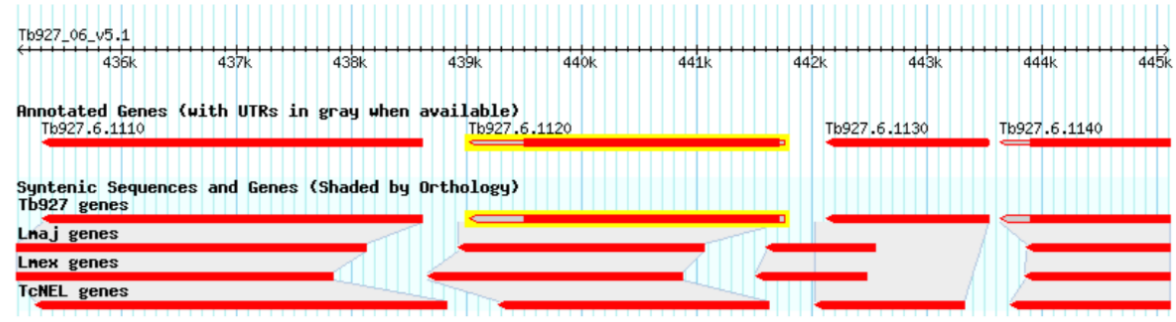

Figure 7.1. *(continued).*

7.2 Protein sequence Alignments

7.2.1 TbORC1/CDC6 alignment with other organisms' Orc1 subunits

The protein sequences for TbORC1/CDC6 (Tb927.11.7216), as well as for the *Trypanosoma cruzi* (TcCLB.508239.10) and *Leishmania major* orthologues (LmjF.28.0030) were retrieved from the TriTrypDB database (http://tritrypdb.org/tritrypdb/). Sequences of the Orc1 subunits of all the other herein represented organisms were obtained from the NCBI Protein Database (http://www.ncbi.nlm.nih.gov/protein), although the protein identification numbering refers to styles used by different databases such as GenBank, InterPro, and NCBI Reference Sequence. Orc1 subunits of model eukaryotes such as human, *Homo sapiens* (HmOrc1, AAC50325.1), domestic mouse, *Mus musculus* (MmOrc1, NP_035145.2), fruit fly, *Drosophila melanogaster* (DmOrc1, NP_477303.1), model plant, *Arabidopsis thaliana* (AtOrc1, NP_567440.1), and the baking yeast, *Saccharomyces cerevisiae* (ScOrc1, NP_013646.1), were used for the alignment. In addition, the sequence for the archaea *Aeropyrum pernix* (ApOrc1, BAA79440.2) Orc1/Cdc6 protein was also used, as this was the sequence used in the first published work on TbORC1/CDC6 and TcORC1/CDC6 factors (Godoy *et al.*, 2009). Alignment was performed and graphically represented using CLC genomics, version 7.5.1 (QIAGEN Aarhus A/S), with a gap open cost of 10.0, a gap extension cost of 1.0, an end gap cost of "as any other", and the very accurate (slow) option for alignment. Results are depicted in Figure 7.2. Regions of high conservation were used to deduce potential motif regions and thus produce the domain and motif schematic representation of TbORC1/CDC6, shown and discussed in Chapter 3, Figure 3.1.

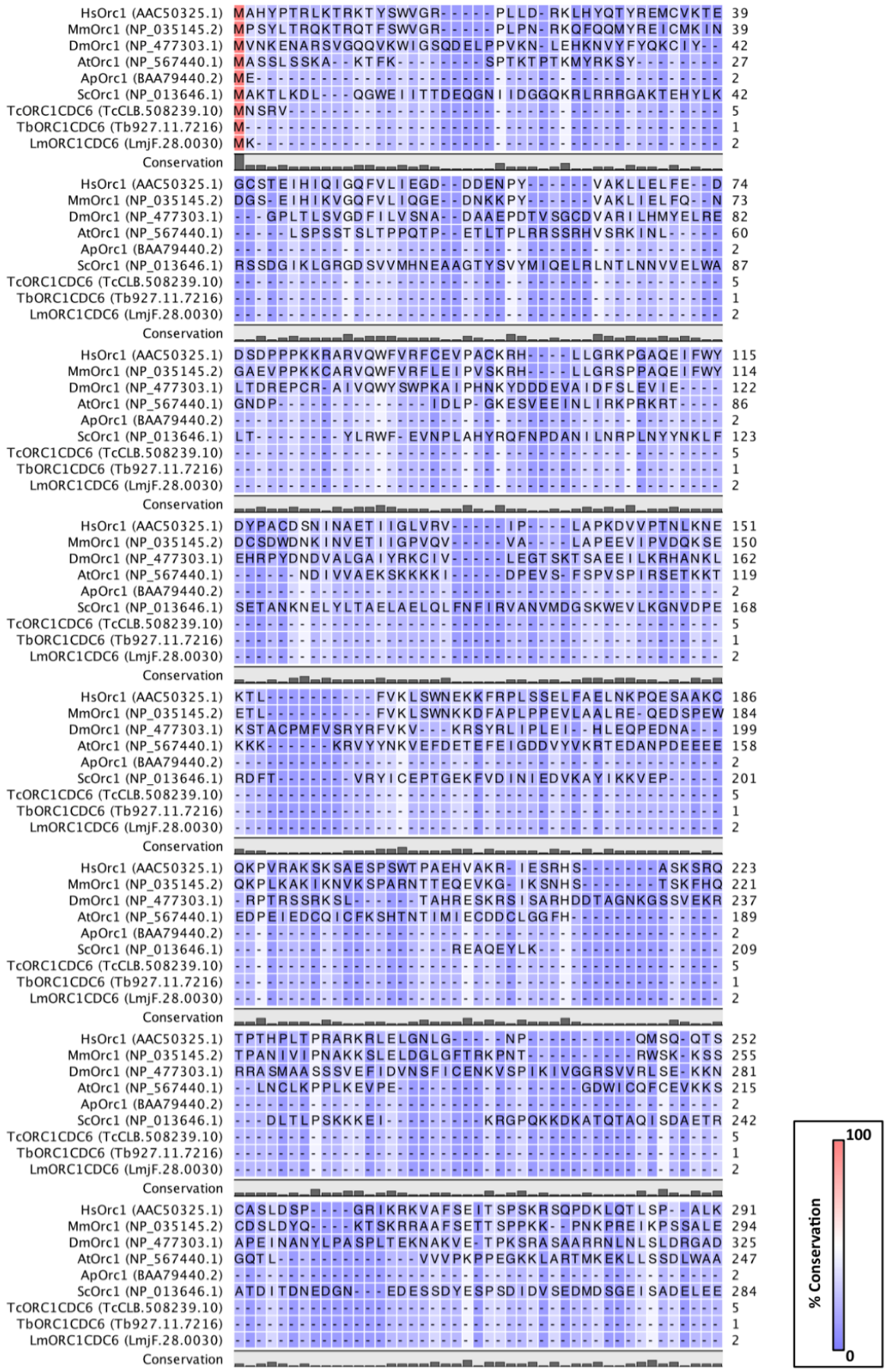

Figure 7.2. Alignment of TbORC1/CDC6 with Orc1 subunits of a range of model organisms. Conservation is depicted by the colour gradient, and sequences are ordered by similarity. Hs, *H. sapiens*; Mm, *M. musculus*; Dm, *D. melanogaster*; At, *A. thaliana*; Ap, *A. pernix*; Sc, *S. cerevisiae*; Tc, *T. cruzi*; Tb, *T. brucei*; Lm, *L. major*. (----) underlines the WHD domain. *(continued below)*

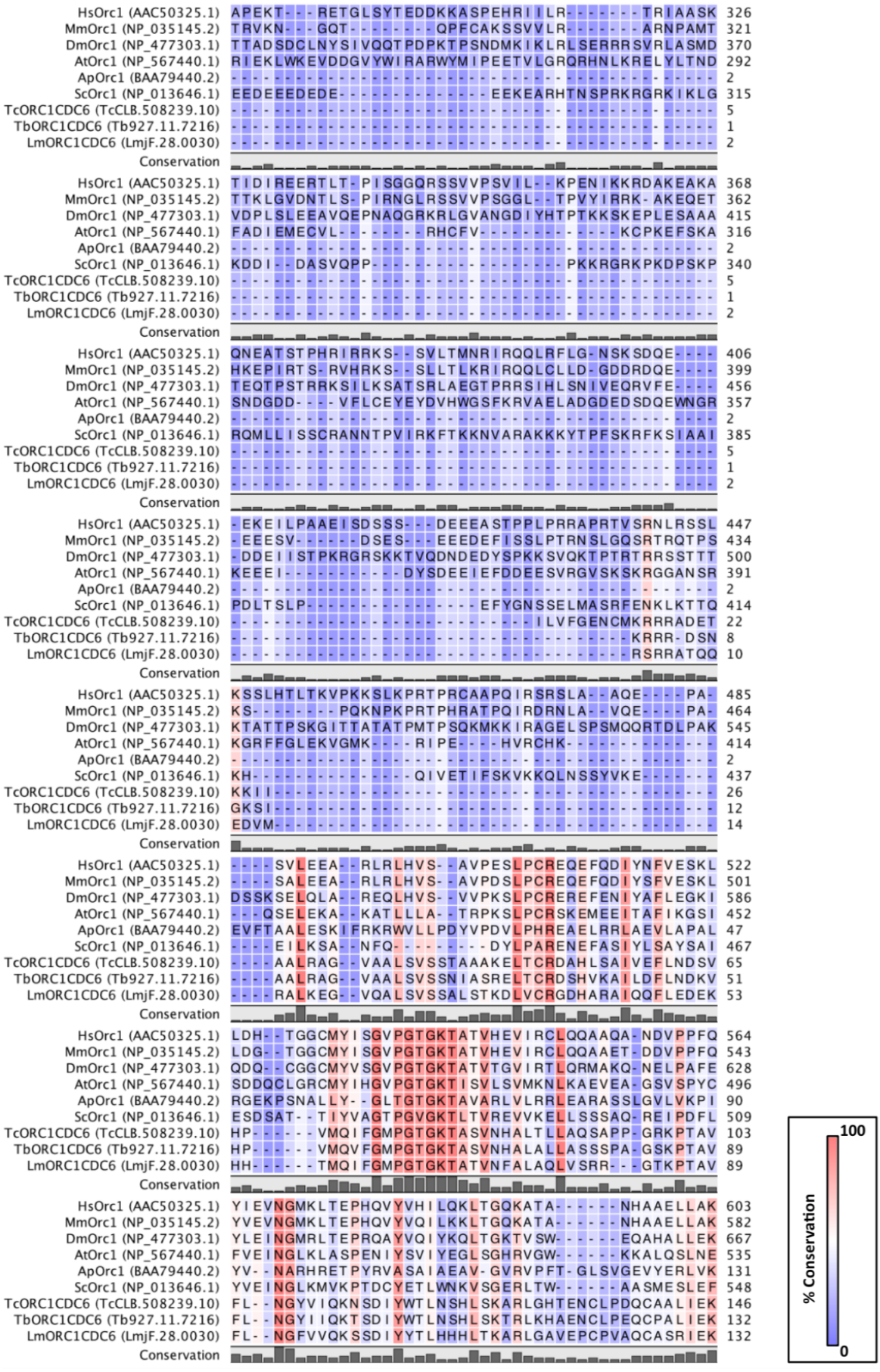

Figure 7.2. *(continued)*

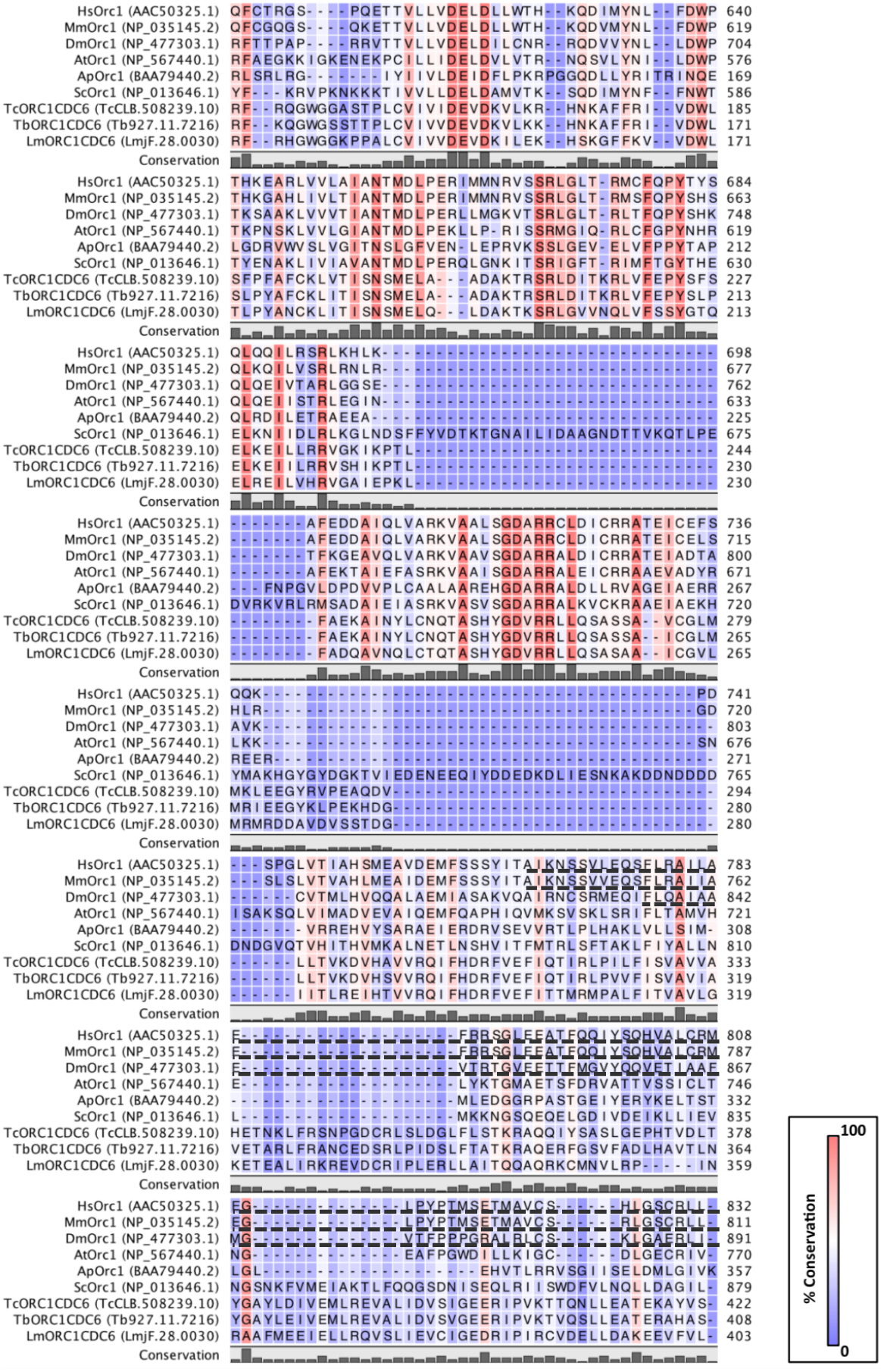

Figure 7.2. *(continued)*

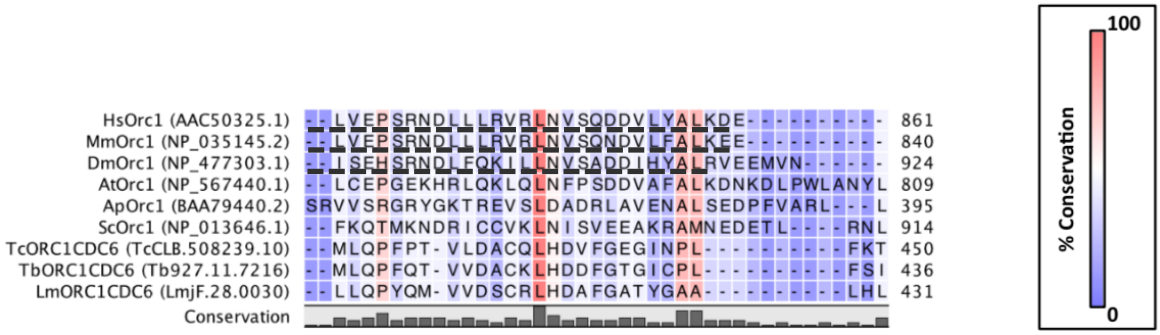

Figure 7.2. *(continued)*

7.2.2 TbORC1B alignment with model eukaryotes' Cdc6 proteins

Protein sequences were retrieved from the appropriate databases, as described in the previous section. For simplicity, the *T. cruzi* and *L. major* orthologues of TbORC1B (Tb927.9.2030) were here represented as TcORC1B (TcCLB.507939.14) and LmORC1B (LmjF.26.2210), respectively. The following Cdc6 protein sequences from model eukaryotes were used for the alignment: *M. musculus* (MmCdc6, NP_035929.1), *H. sapiens* (HsCdc6, NP_001245.1), *D. melanogaster* (DmCdc6, AAF50387.1), *A. thaliana* (AtCdc6, AEC08293.1), and *S. cerevisiae* (ScCdc6, CAA89490.1). In addition, the Cdc6 protein of *Clonorchis sinensis* (CsCdc6, GAA29103.2) was also used, as this was the first hit obtained when using TbORC1B as a query in blastp (see Chapter 3, section 3.1.2). The alignment was performed as described in the previous section, and the results are represented in Figure 7.3. Regions of high conservation were used to deduce potential motif regions and thus produce the domain and motif schematic representation of TbORC1B, shown and discussed in Chapter 3, Figure 3.1.

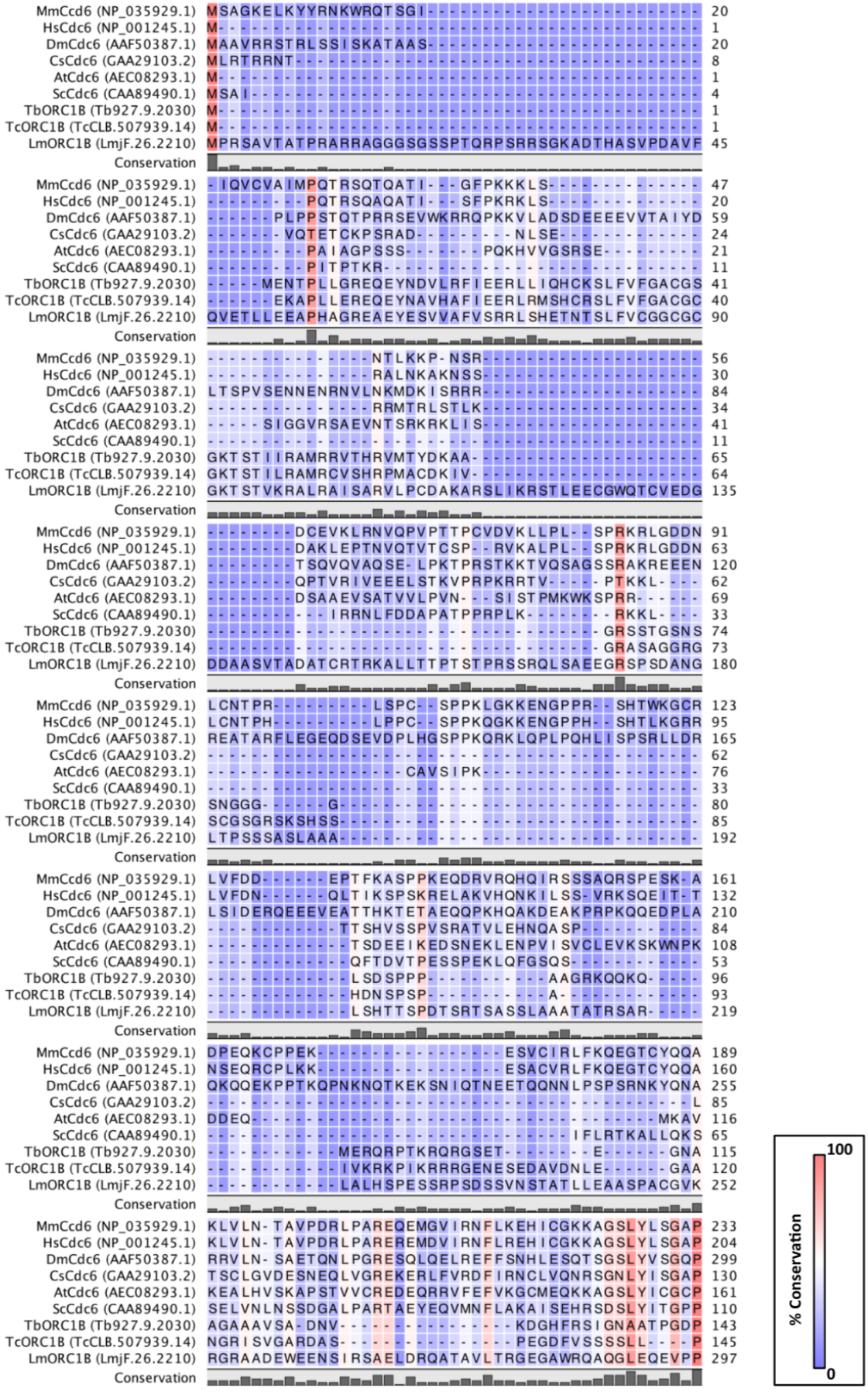

Figure 7.3. Alignment of TbORC1B with Cdc6 proteins of a range of model eukaryotes. Conservation is depicted by the colour gradient, and sequences are ordered by similarity. Mm, *M. musculus*; Hs, *H. sapiens*; Dm, *D. melanogaster*; Cs, *Clonorchis sinensis*; At, *A. thaliana*; Sc, *S. cerevisiae*; Tb, *T. brucei*; Tc, *T. cruzi*; Lm, *L. major*. (----) underlines the WHD domain.*(continued below)*

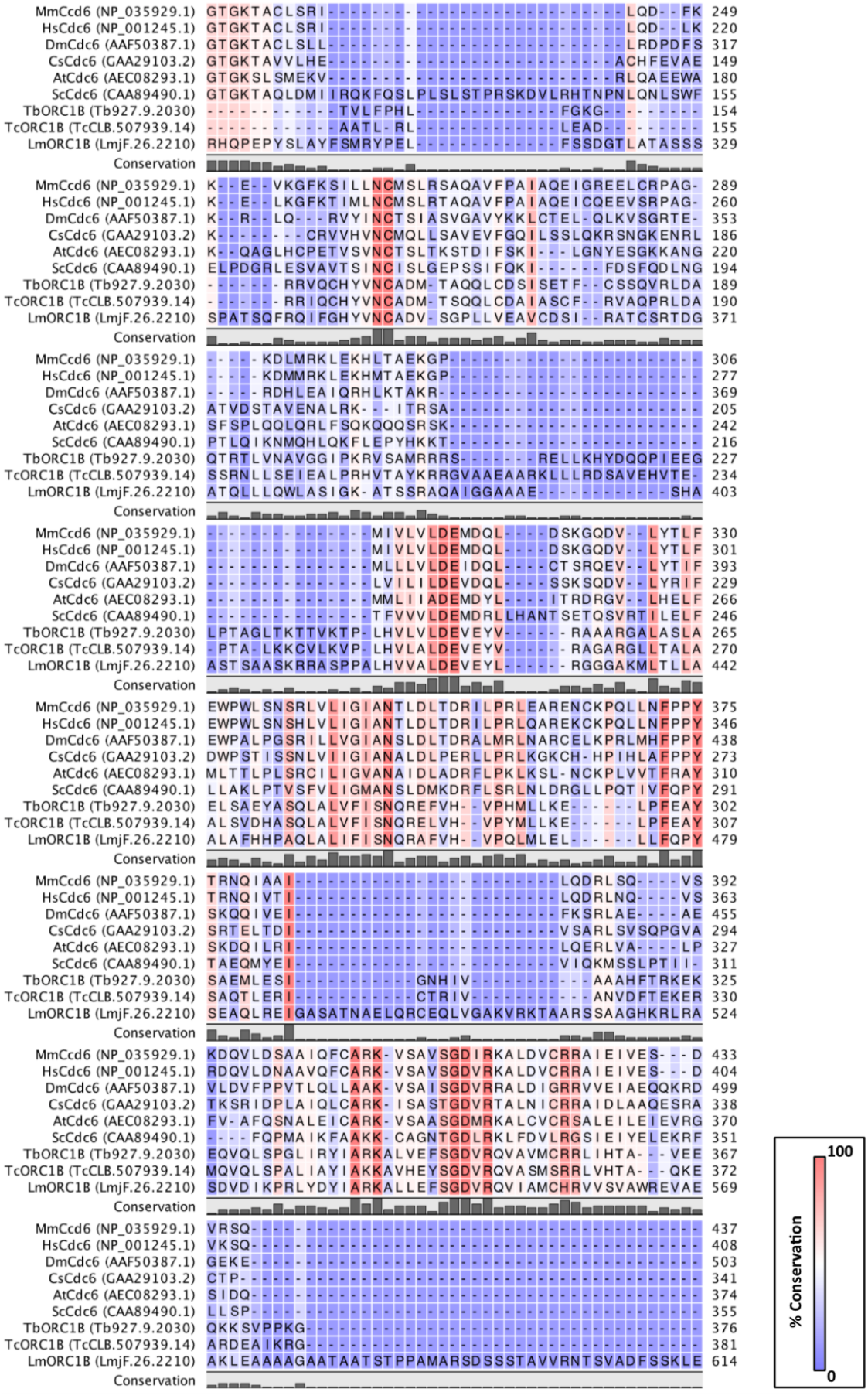

Figure 7.3. *(continued).*

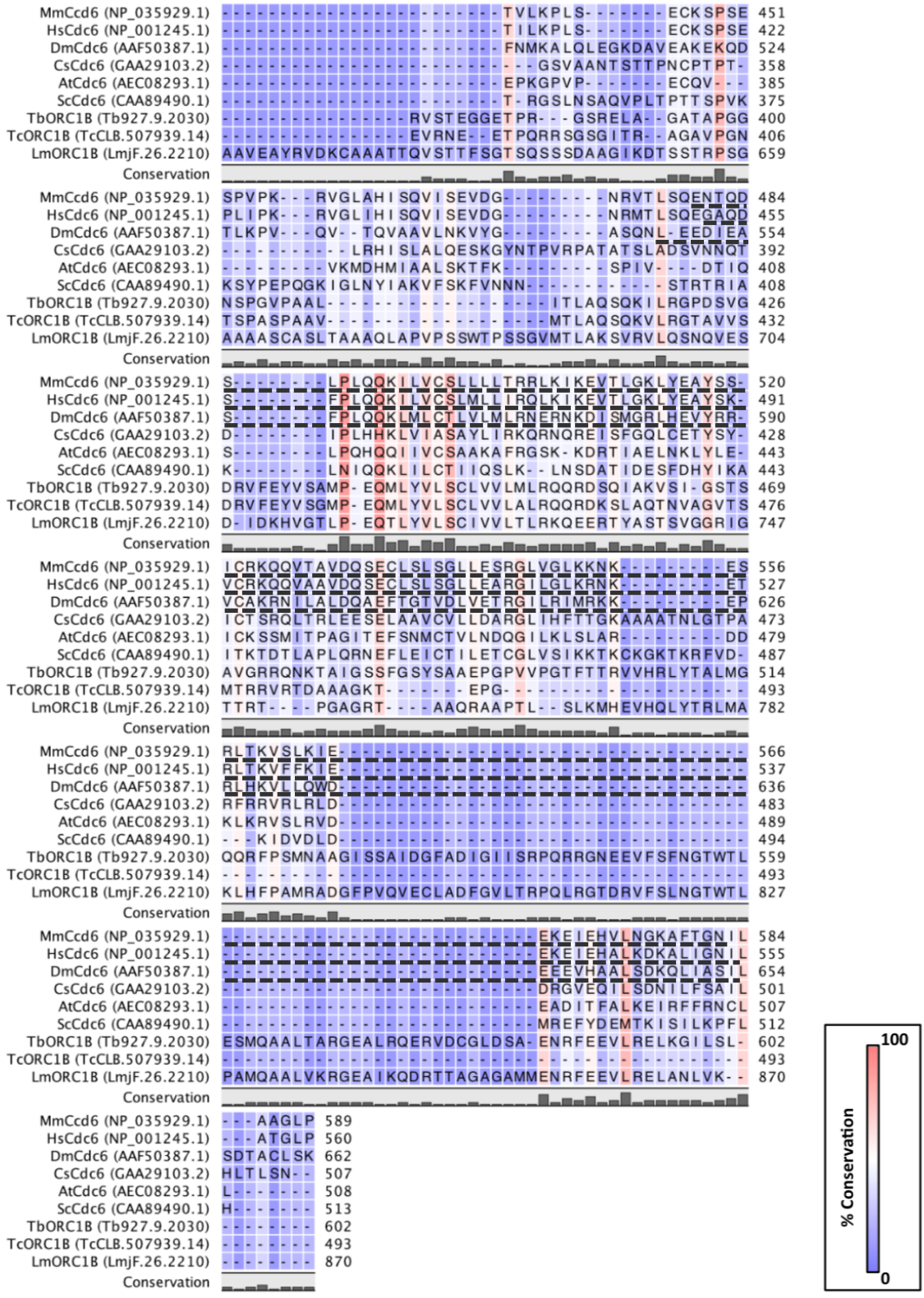

Figure 7.3. *(continued).*

7.2.3 TbORC4 alignment against Orc4 subunits of model eukaryotes

Protein sequences were retrieved from the appropriate databases, as described in section 7.2.1. For simplicity, the *T. cruzi* and *L. major* orthologues of TbORC4 (Tb927.10.13380) were here represented as TcORC4 (TcCLB.506357.20) and LmORC4 (LmjF.18.0720), respectively. The following Orc4 protein sequences from model eukaryotes were used for the alignment: *D. melanogaster* (DmOrc4, AAD39473.1), *H. sapiens* (HsOrc4, NP_001177808.1), *M. musculus* (MmOrc4, CAA76188.1), *A. thaliana* (AtOrc4, AEC05404.1), and *S. cerevisiae* (ScOrc4, AAB68149.1). The Orc4 subunit from *Musca domestica* (MdOrc4, XP_005179312.1) was also used in the alignment, as this was one of the top hits in the blastp analysis performed using TbORC4 as query (see Chapter 3, section 3.1.2). The alignment was performed as described in section 7.2.1, and the results are represented in Figure 7.4. Regions of high conservation were used to infer potential motif regions and thus generate the domain and motif schematic representation of TbORC4, shown and discussed in Chapter 3, Figure 3.1.

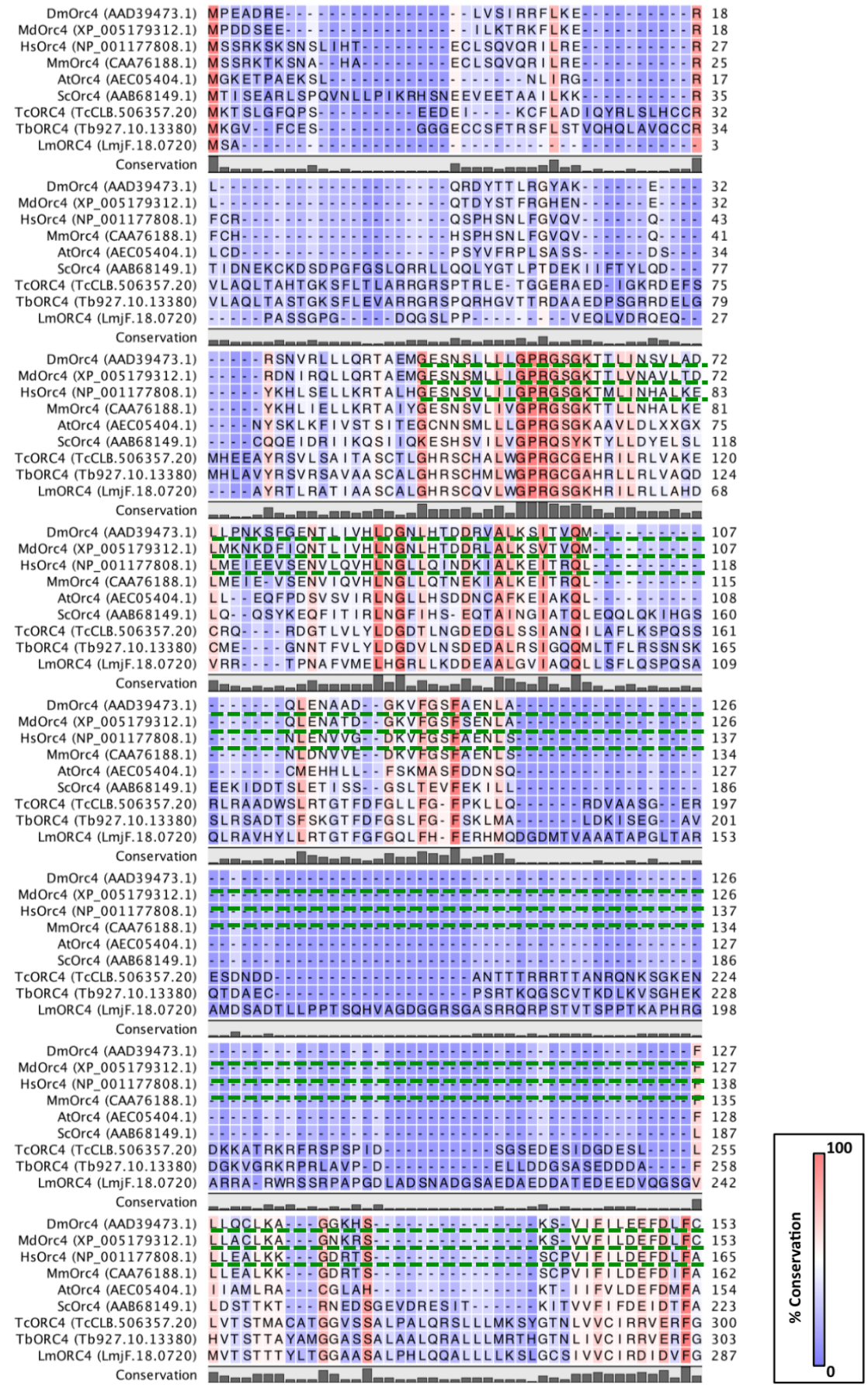

Figure 7.4. TbORC4 alignment with Orc4 subunits of a range of eukaryotes.
Conservation is depicted by the colour gradient, and sequences are ordered by similarity. Dm, *D. melanogaster*; Md, *Musca domestica*; Hs, *H. sapiens*; Mm, *M. musculus*; At, *A. thaliana*; Sc, *S. cerevisiae*; Tc, *T. cruzi*; Tb, *T. brucei*; Lm, *L. major*. (----) underlines the AAA+ ATPase domain. *(continued below)*

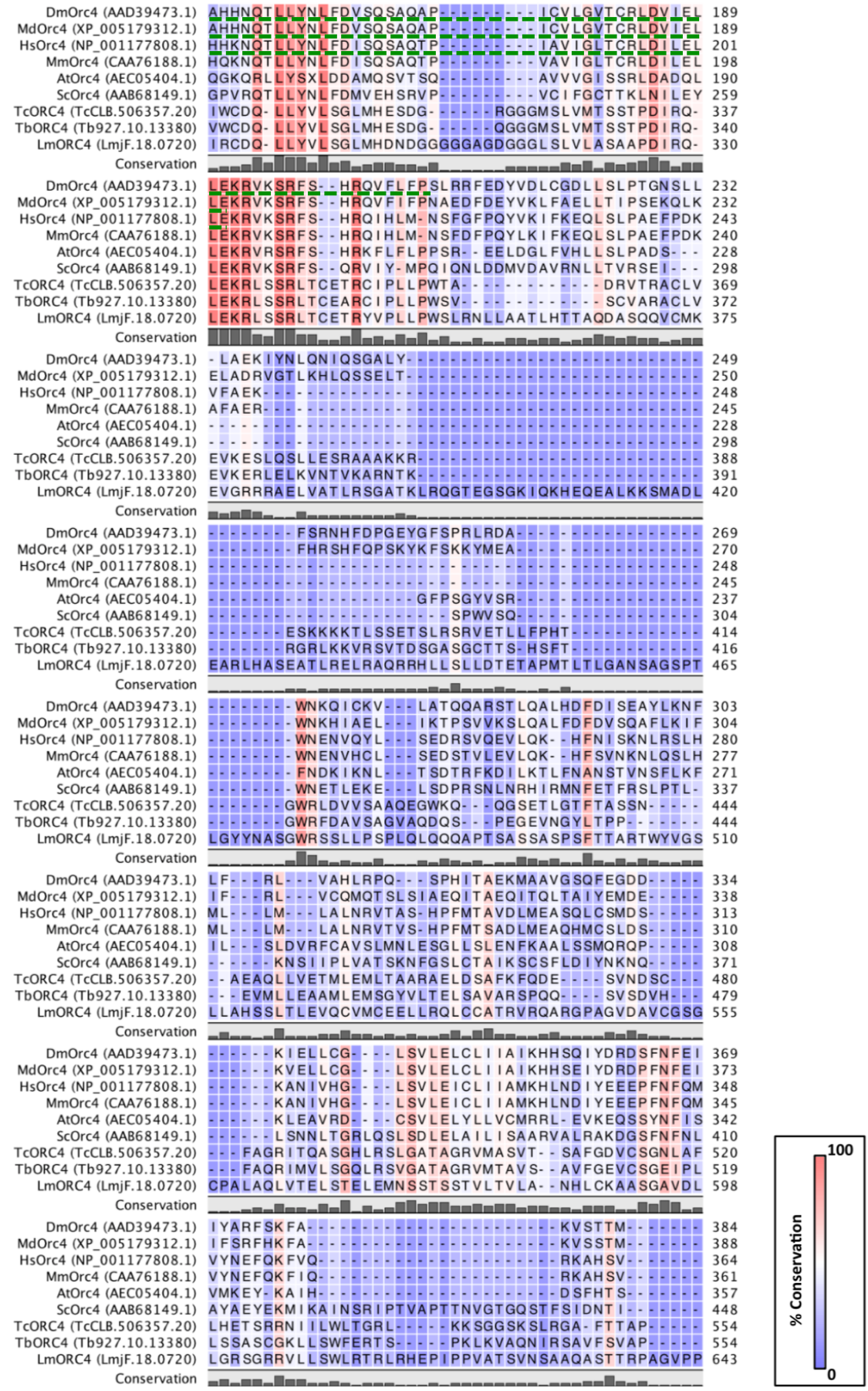

Figure 7.4. *(continued).*

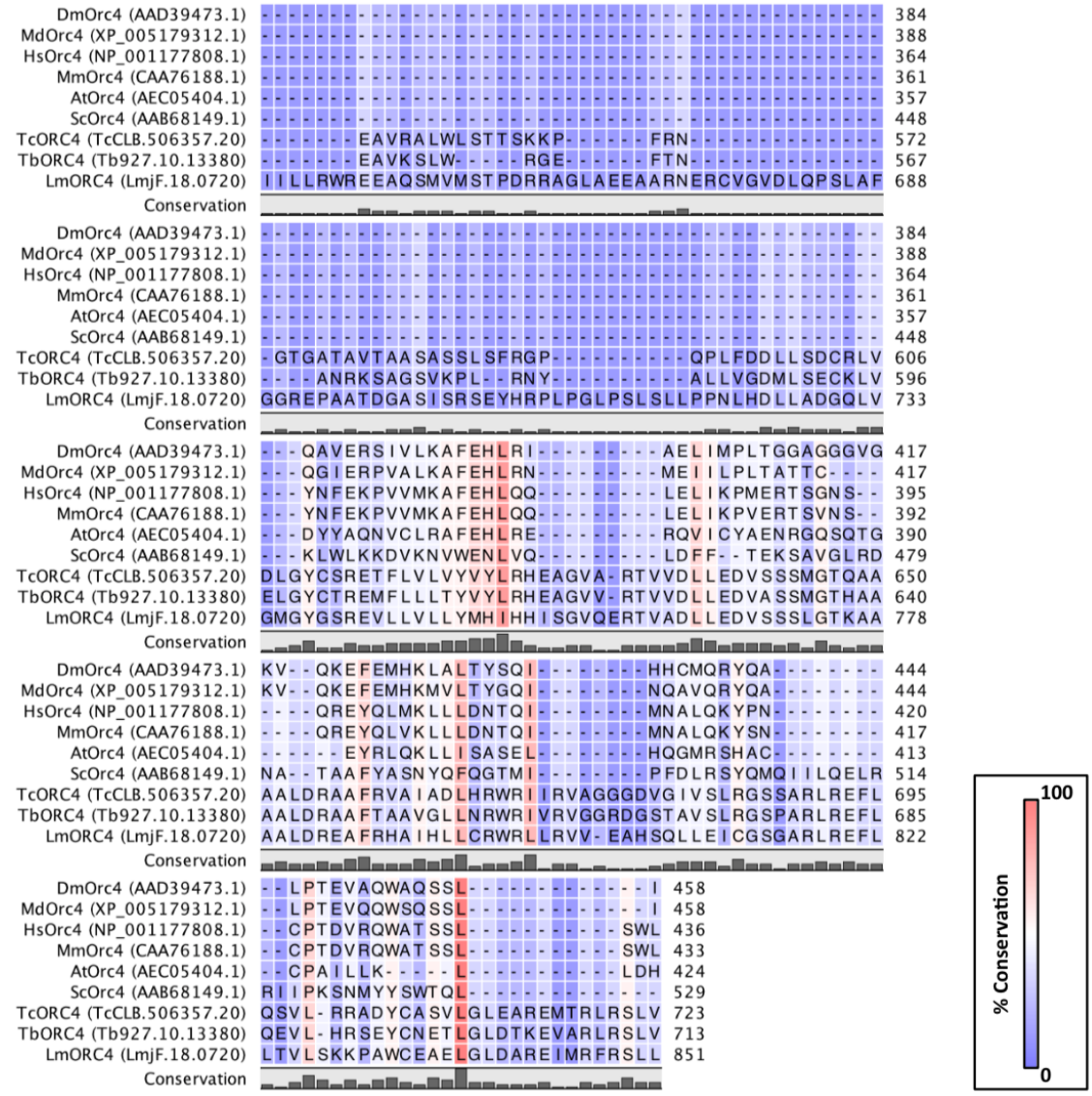

Figure 7.4. *(continued).*

7.2.4 Tb7980 alignment against Orc5 subunits of model eukaryotes

Protein sequences were retrieved from the appropriate databases, as described in section 7.2.1. *T. cruzi* and *L. major* orthologues of Tb7980 (Tb927.10.7980) were here represented as Tc7980 (TcCLB.506247.280) and Lm7980 (LmjF.36.6700), respectively. The following Orc5 protein sequences from model eukaryotes were used for the alignment: *H. sapiens* (HsOrc5, NP_002544.1), *M. musculus* (MmOrc5, NP_036089.1), *D. melanogaster* (DmOrc5, NP_477132.1), *A. thaliana* (AtOrc5, NP_194720.2), and *S. cerevisiae* (ScOrc5, CAA65483.1). The alignment was performed as described in section 7.2.1, and the results are represented in Figure 7.5. Regions of high conservation were used to infer potential motif regions and thus generate the domain and motif schematic representation of Tb7980, shown and discussed in Chapter 3, Figure 3.1.

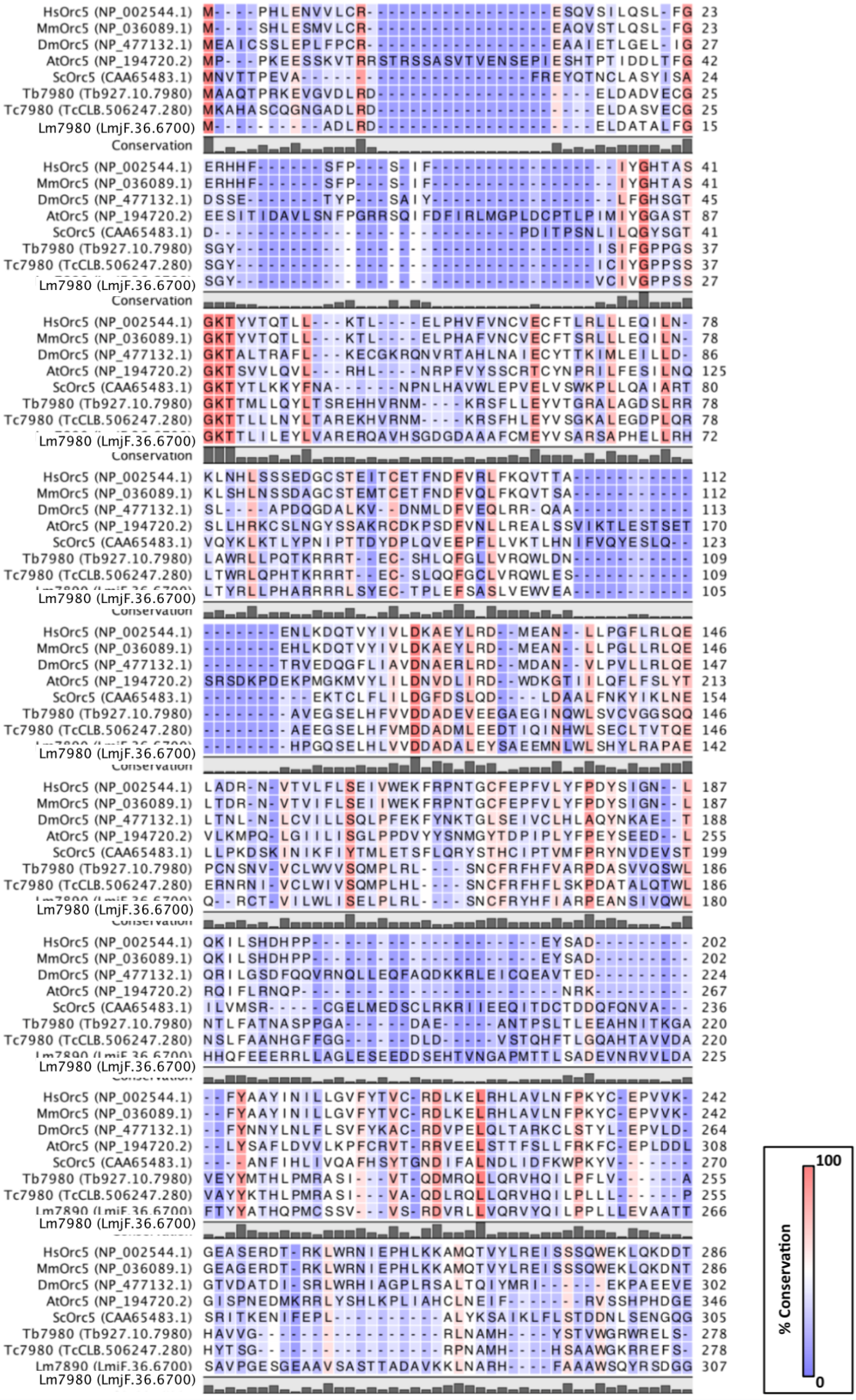

Figure 7.5. Tb7980 alignment with Orc5 subunits of model eukaryotes.
Conservation is depicted by the colour gradient. Hs, H. sapiens; Mm, M. musculus; Dm, D. melanogaster; At, A. thaliana; Sc, S. cerevisiae; Tb, T. brucei; Tc, T. cruzi; Lm, L. major. (continued below)

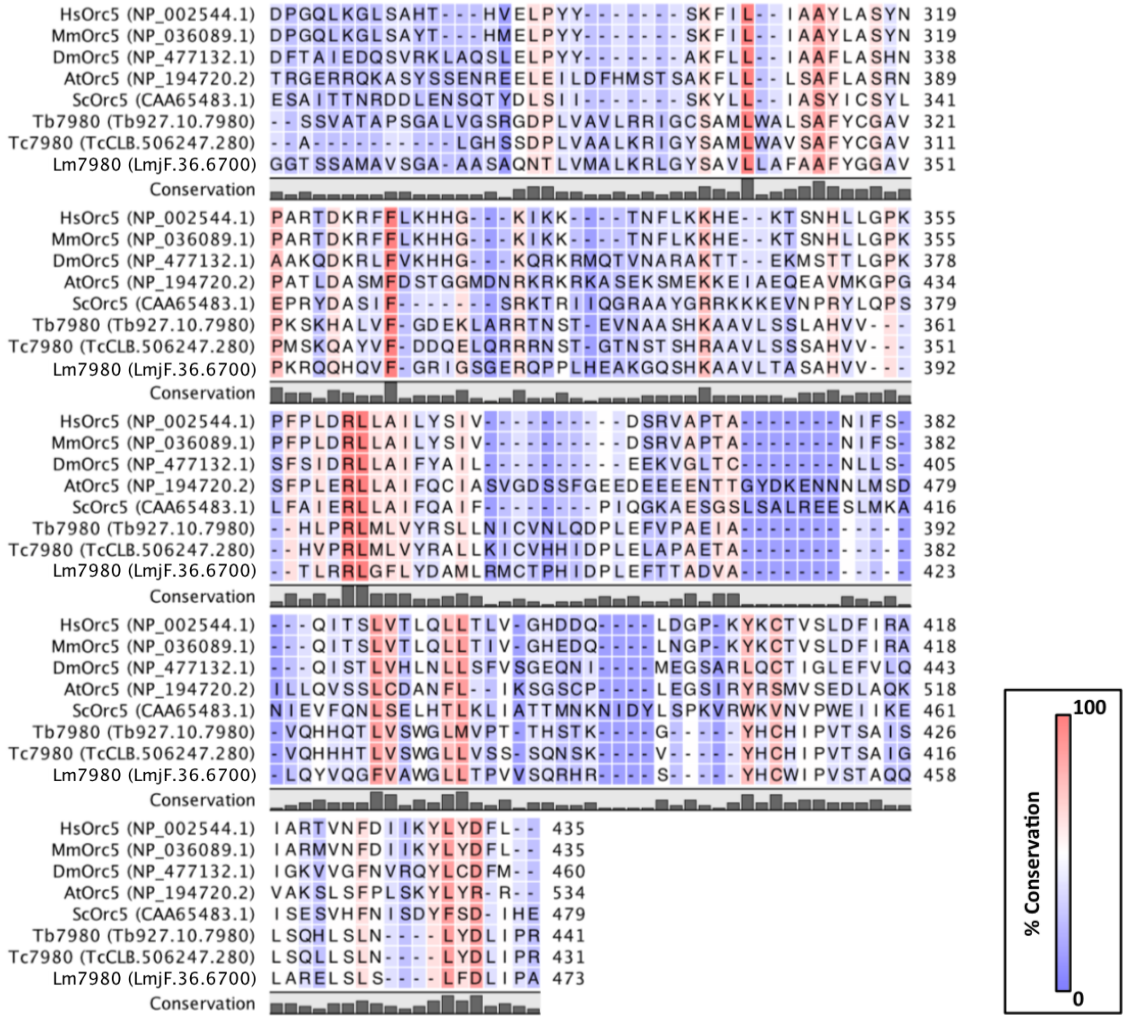

Figure 7.5. *(continued)*.

7.2.5 Tb3120 alignment against model eukaryotes Orc2 subunits

Protein sequences were retrieved from the appropriate databases, as described in section 7.2.1. *T. cruzi* and *L. major* orthologues of Tb3120 (Tb927.9.4530) were here represented as Tc3120 (TcCLB.511585.90) and Lm3120 (LmjF.01.0660), respectively. The following Orc2 protein sequences from model eukaryotes were used for the alignment: *H. sapiens* (HsOrc2, NP_006181.1), *M. musculus* (MmOrc2, Q60862.1), *D. melanogaster* (DmOrc2, AAF99606.1), *A. thaliana* (AtOrc2, AEC09416.1), and *S. cerevisiae* (ScOrc2, CAA85003.1). The alignment was performed as described in section 7.2.1, and the results are represented in Figure 7.6. Regions of high conservation were used to infer potential motif regions and thus generate the domain and motif schematic representation of Tb3120, shown and discussed in Chapter 3, Figure 3.1.

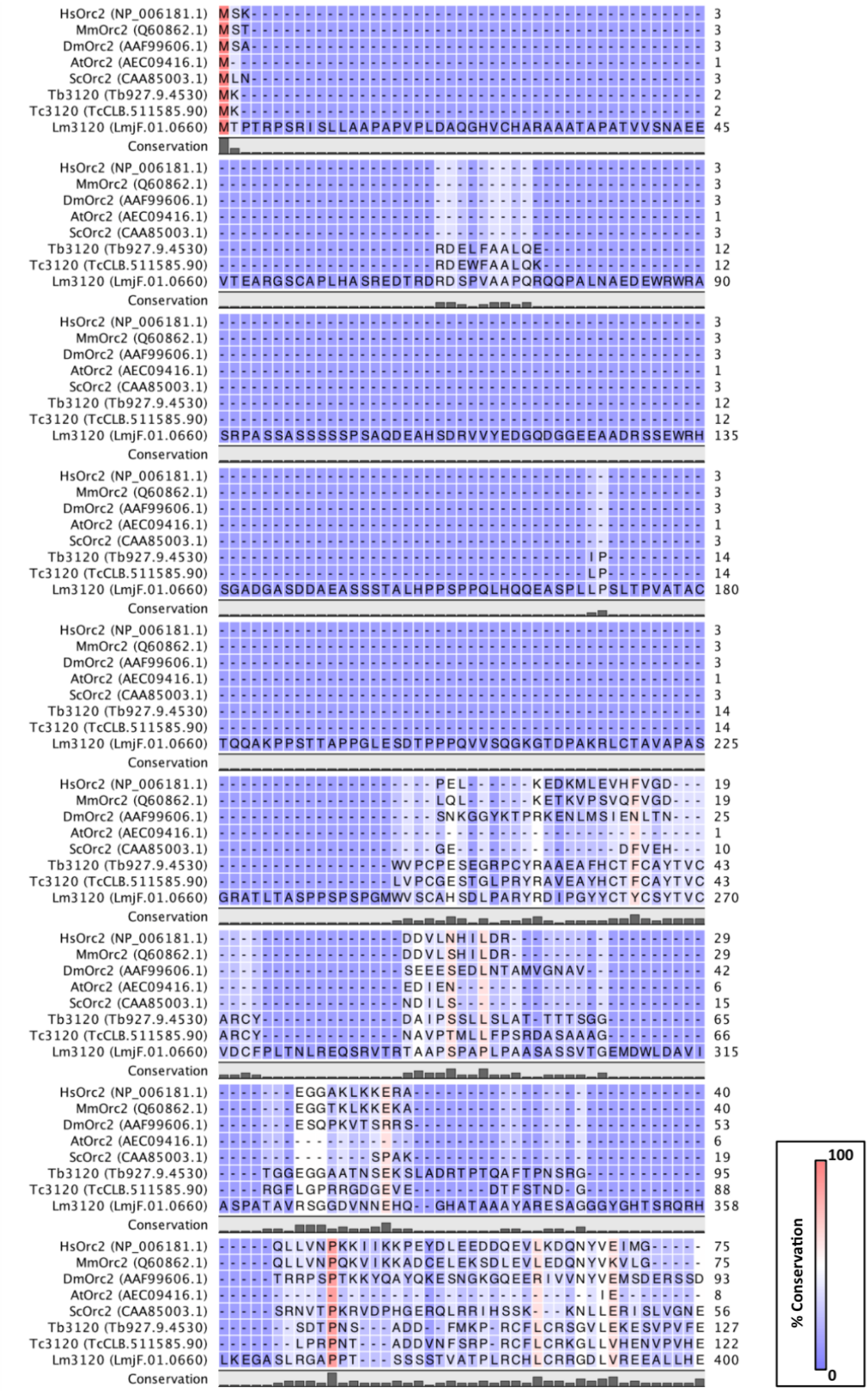

Figure 7.6. Alignment of Tb3120 with Orc2 subunits from model eukaryotes. Conservation is depicted by the colour gradient. Hs, *H. sapiens*; Mm, *M. musculus*; Dm, *D. melanogaster*; At, *A. thaliana*; Sc, *S. cerevisiae*; Tb, *T. brucei*; Tc, *T. cruzi*; Lm, *L. major*. Potential Walker A and Walker B motifs are shown within the dashed green boxes. *(continued below)*

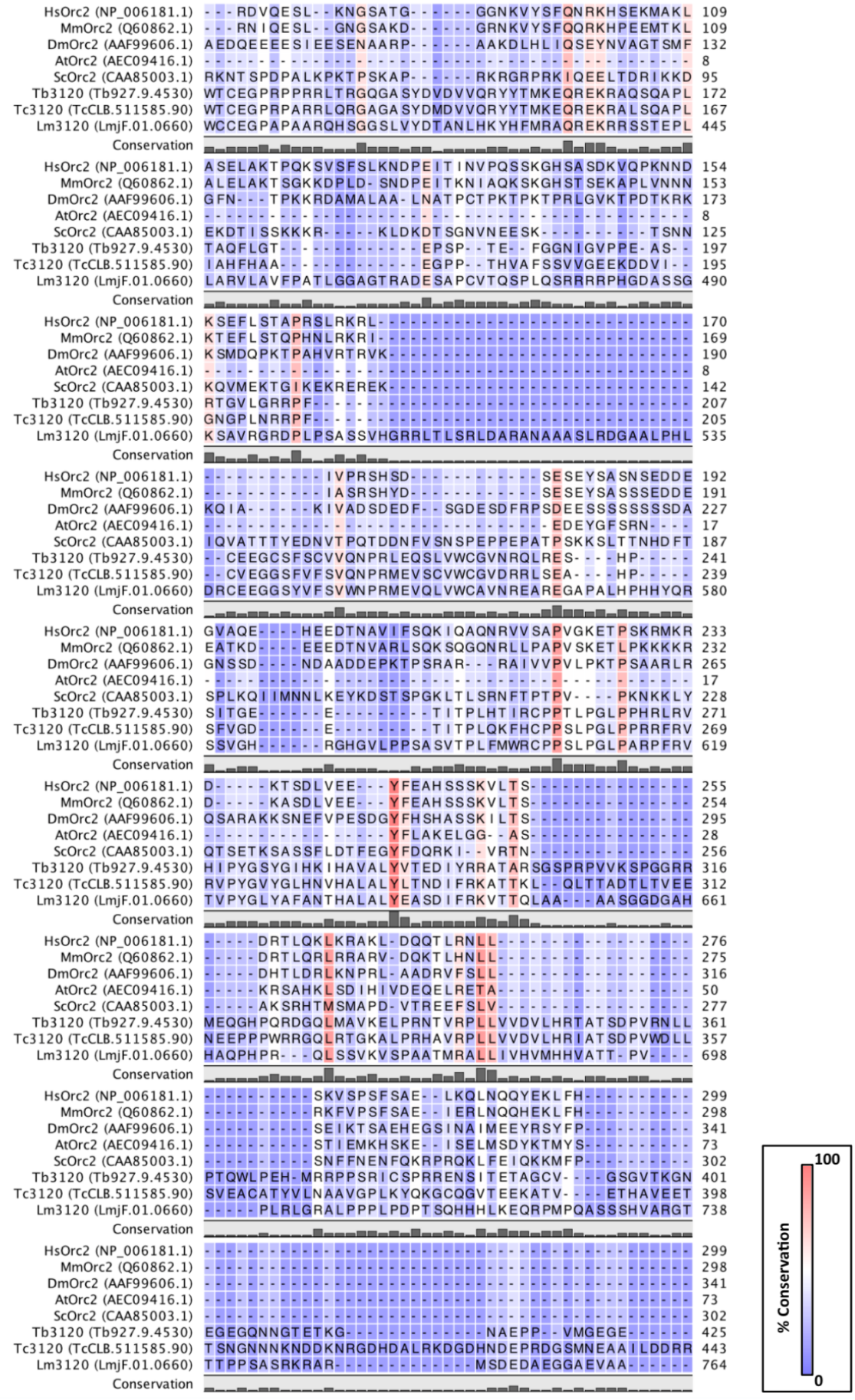

Figure 7.6. *(continued)*.

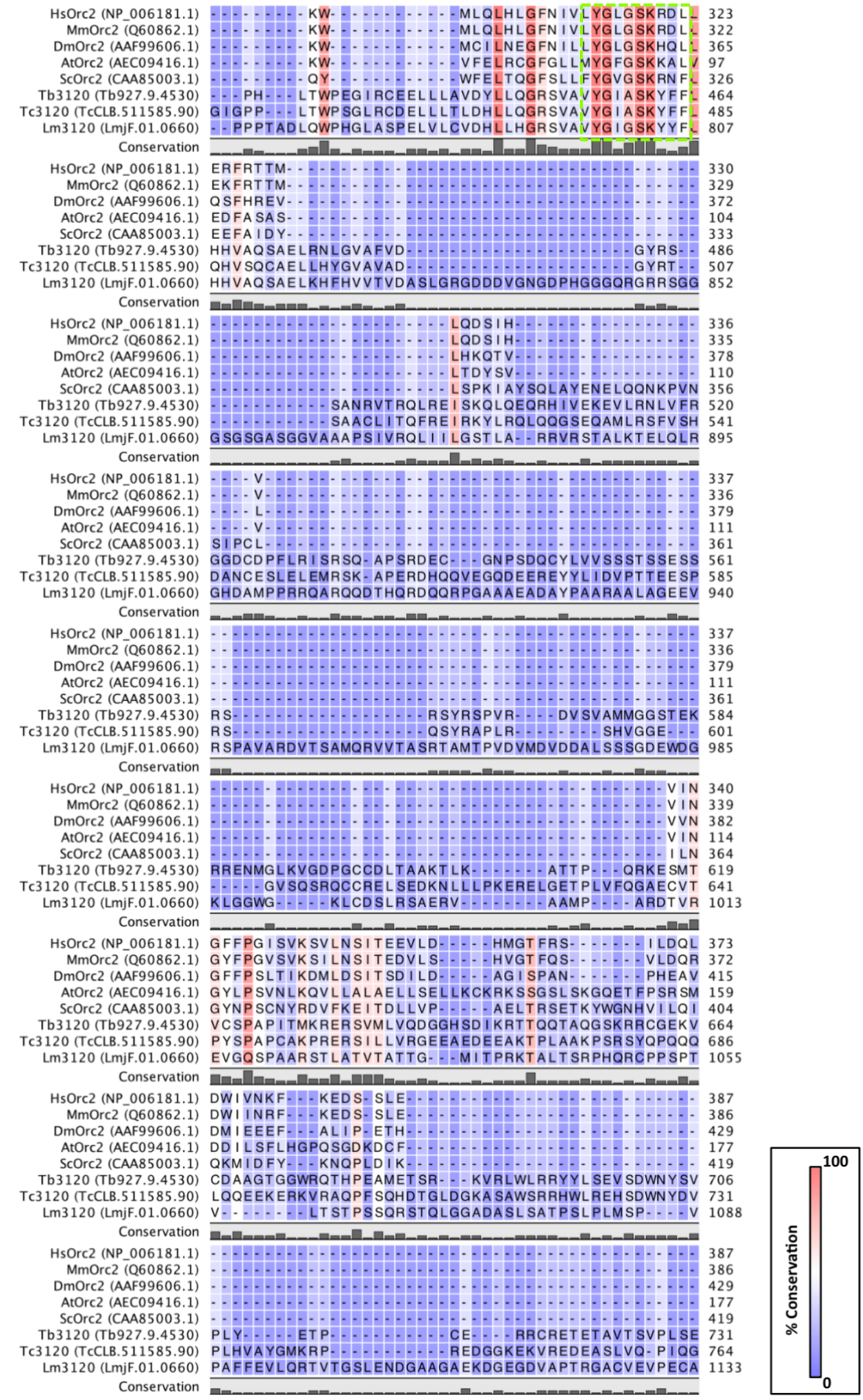

Figure 7.6. *(continued)*.

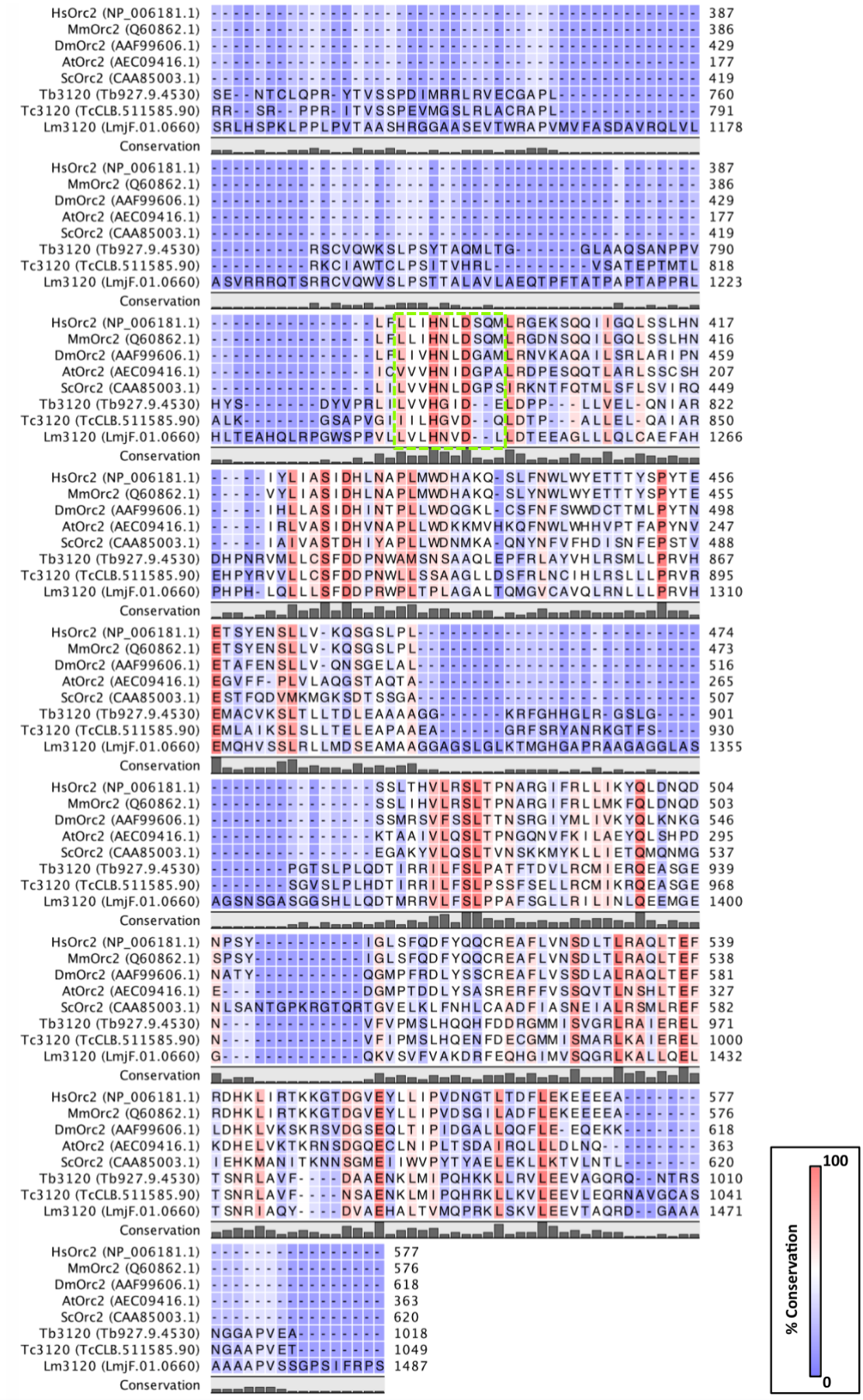

Figure 7.6. *(continued)*.

7.3 RNAi in PCF cells

These results refer to the results shown in Chapter 3, section 3.3.2.

7.3.1 Extra TbORC1/CDC6 and Tb3120 RNAi clones

Here are shown the results for two clones, TbORC1/CDC6 RNAi Cla (Figure 7.7) and Tb3120 RNAi Cla (Figure 7.8) that revert the RNAi phenotype after 72 h and 168 h post-induction, respectively.

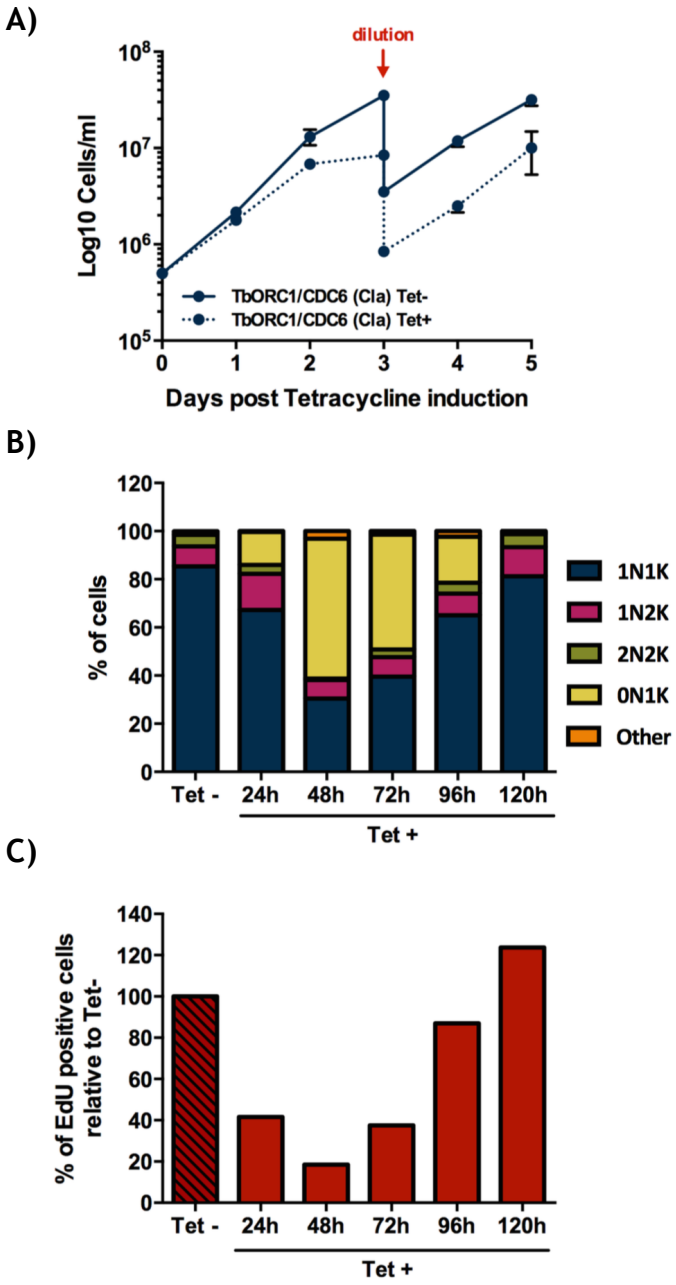

Figure 7.7. Effect of TbORC1/CDC6 depletion by induction of specific gene targeted RNAi over time.

A) Growth curves of un-induced (Tet -) and tetracycline-RNAi induced (Tet +) cell cultures over five days. Cell concentration was assessed every 24 h, and plotted on a Log_{10} y-axis graph. The individual points represent the mean from two independent experiments, while the error bars depict the standard error of the mean (SEM). The red arrow pinpoints a 1:10 dilution of both Tet – and Tet + cultures. B) Quantification of cells in the different cell cycle stages throughout the course of five days of RNAi induction, based on the nuclear and kinetoplast configuration of the cells stained with DAPI. A minimum of 150 cells was counted per time point and experimental group (Tet - and Tet +), and percentages of each cell type (1N1K, 1N2K, 2N2K, 0N1K, and others) were calculated relative to the total amount of cells analysed. Only one experiment is shown. C) Percentage of EdU positive cells in the Tet + samples relative to the percentage of EdU positive cells in the Tet - culture from the same time point. A minimum of 150 cells were analysed per time point and group (Tet - and Tet +). Only one experiment is shown.

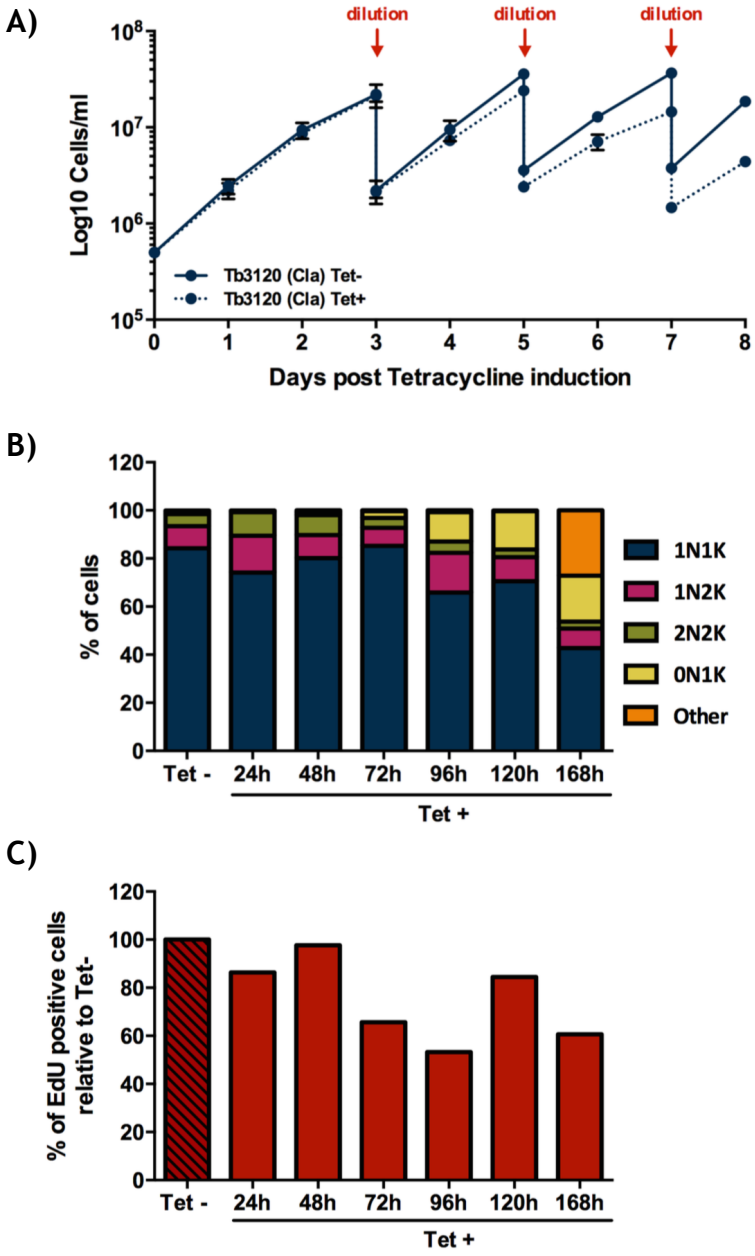

Figure 7.8. Effect of Tb3120 depletion by induction of specific gene targeted RNAi over time. A) Growth curves of un-induced (Tet -) and tetracycline-RNAi induced (Tet +) cell cultures over eight days. Cell concentration was assessed every 24 h, and plotted on a Log_{10} y-axis graph. The individual points represent the mean from two independent experiments, while the error bars depict the standard error of the mean (SEM). The red arrow pinpoints a 1:10 dilution of both Tet – and Tet + cultures. B) Quantification of cells in the different cell cycle stages throughout the course of five

days of RNAi induction, based on the nuclear and kinetoplast configuration of the cells stained with DAPI. A minimum of 150 cells was counted per time point and experimental group (Tet - and Tet +), and percentages of each cell type (1N1K, 1N2K, 2N2K, 0N1K, and others) were calculated relative to the total amount of cells analysed. Only one experiment is shown. C) Percentage of EdU positive cells in the Tet + samples relative to the number of EdU positive cells in the Tet - culture from the same time point. A minimum of 150 cells were analysed per time point and group (Tet - and Tet +). Only one experiment is shown.

7.3.2 Flow cytometry analysis of the effects on cell cycle resultant from gene-targeted RNAi induction

Here are shown the individual DNA content histograms obtained from flow cytometry analysis of the RNAi-induced cell lines, and used to generate the graphs in Chapter 3, Figure 3.11.

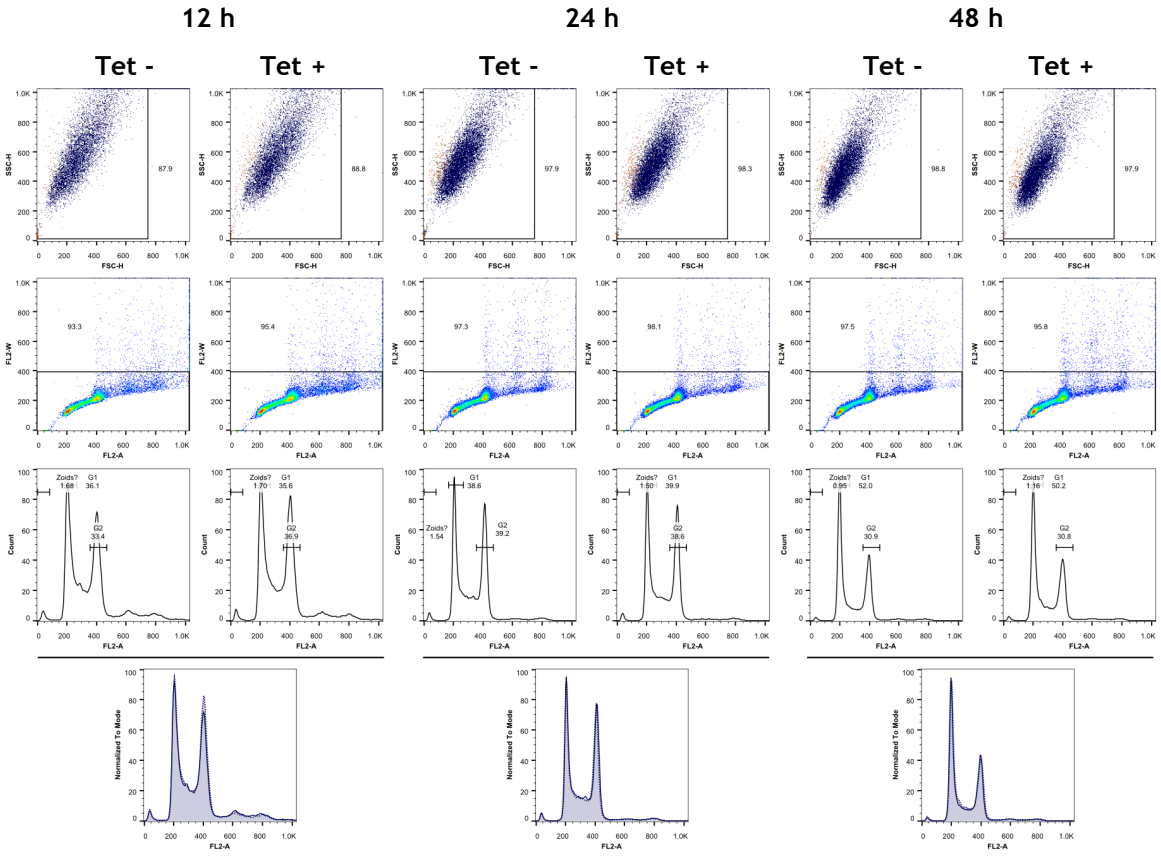

Figure 7.9. 2913 cell line, 12 h, 24 h and 48 h time points.
Top row, scatter plots of the side scatter (SSC) x forward scatter (FSC), showing the cells in the population by internal complexity (SSC) and size (FSC). The gate is shown as a rectangle enclosing the whole cellular population; the percentage of cells within is shown. These cells are shown in the row below, displayed in scatter plots of FL2-W (width) x FL2-A (area), as FL2 is the detector that detects the propidium iodide fluorescent signal. The gate is shown as a rectangle, and the percentage of cells within is shown. The graphs below represent the cells within that gate but as histograms of the FL2-A data. Here, gates are shown for the G1 and G2 populations, as well as a sub-G1 population labelled as zoids. The percentages for each are shown, and these were used to generate the graph in Chapter 3, Figure 3.11. Using the back-gating function of FlowJo, the "zoid" population was back-gated to the SSCxFSC plot, and the cells are shown in orange. Bottom graphs show the overlap of the histograms of the Tet – (full blue line) and Tet + (dashed blue line) samples for each time point.

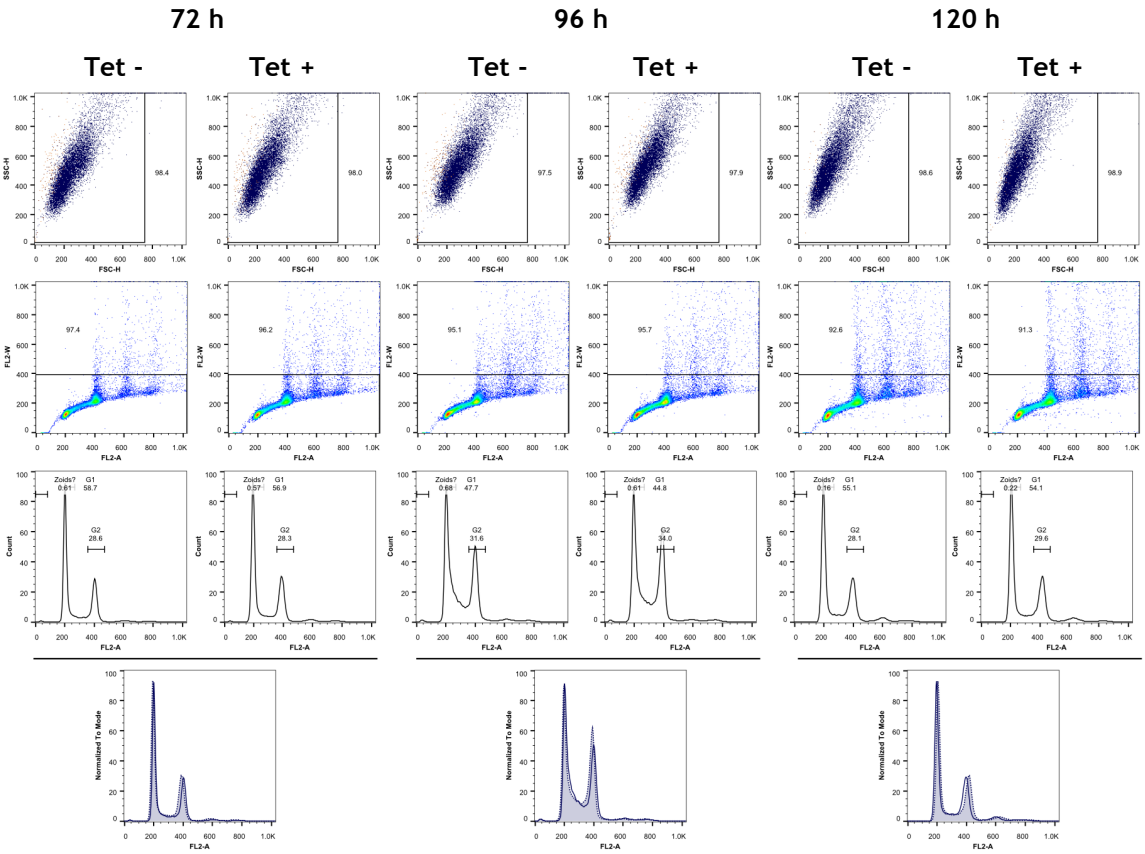

Figure 7.10. 2913 cell line, 72 h, 96 h and 120 h time points.
Description as in Figure 7.9.

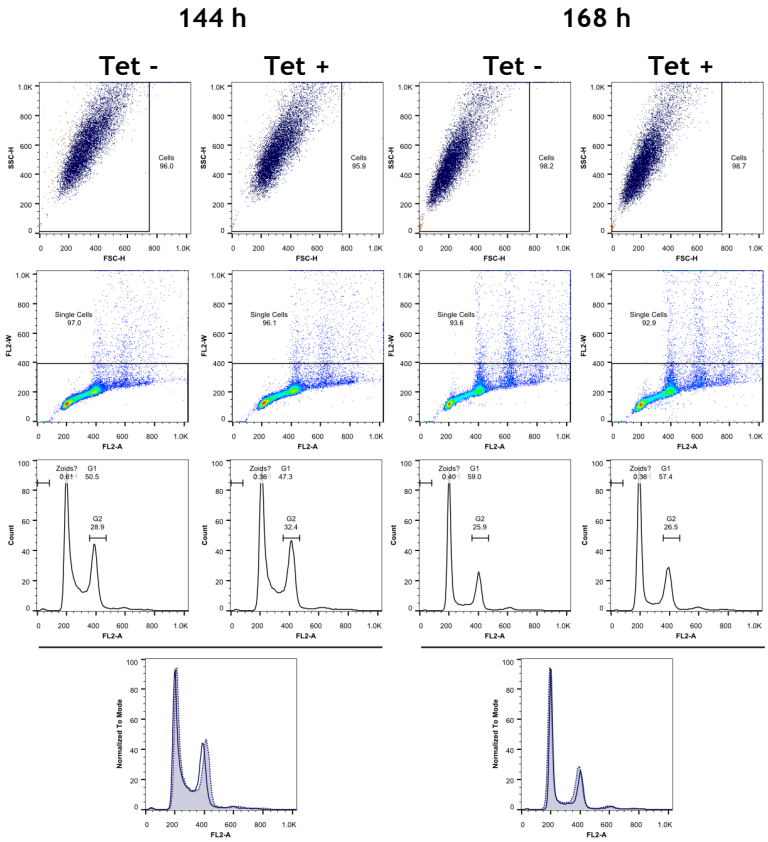

Figure 7.11. 2913 cell line, 144 h and 168 h time points.
Description as in Figure 7.9.

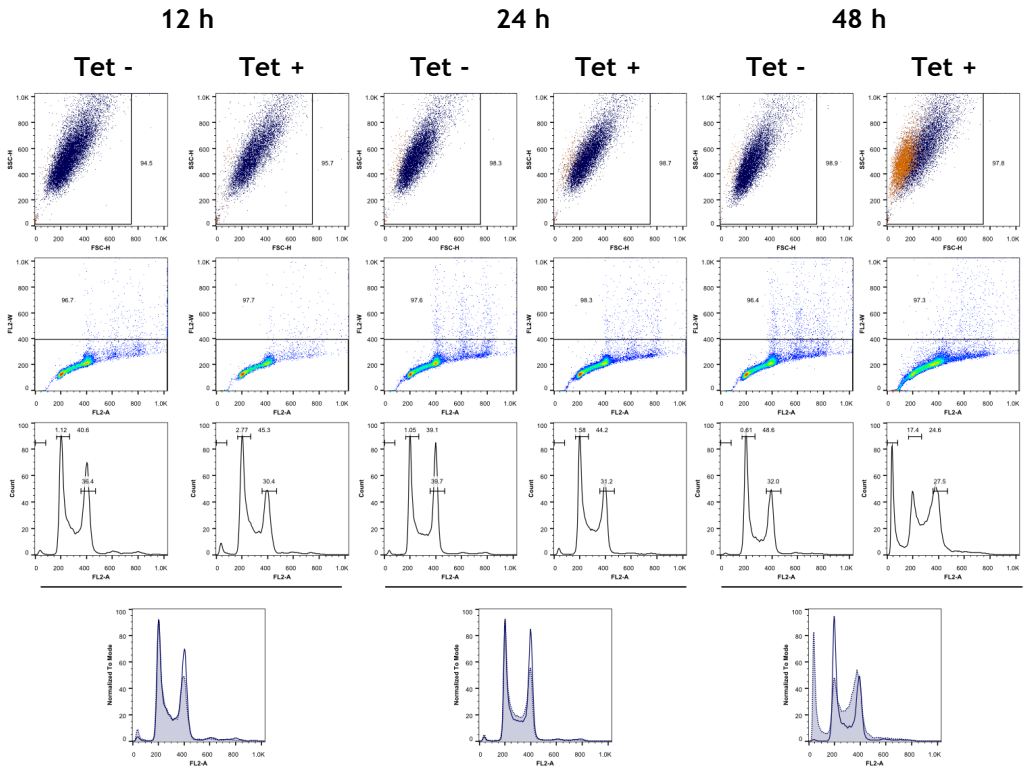

Figure 7.12. TbORC1/CDC6 RNAi Clb cell line, 12 h, 24 h and 48 h time points.
Description as in Figure 7.9.

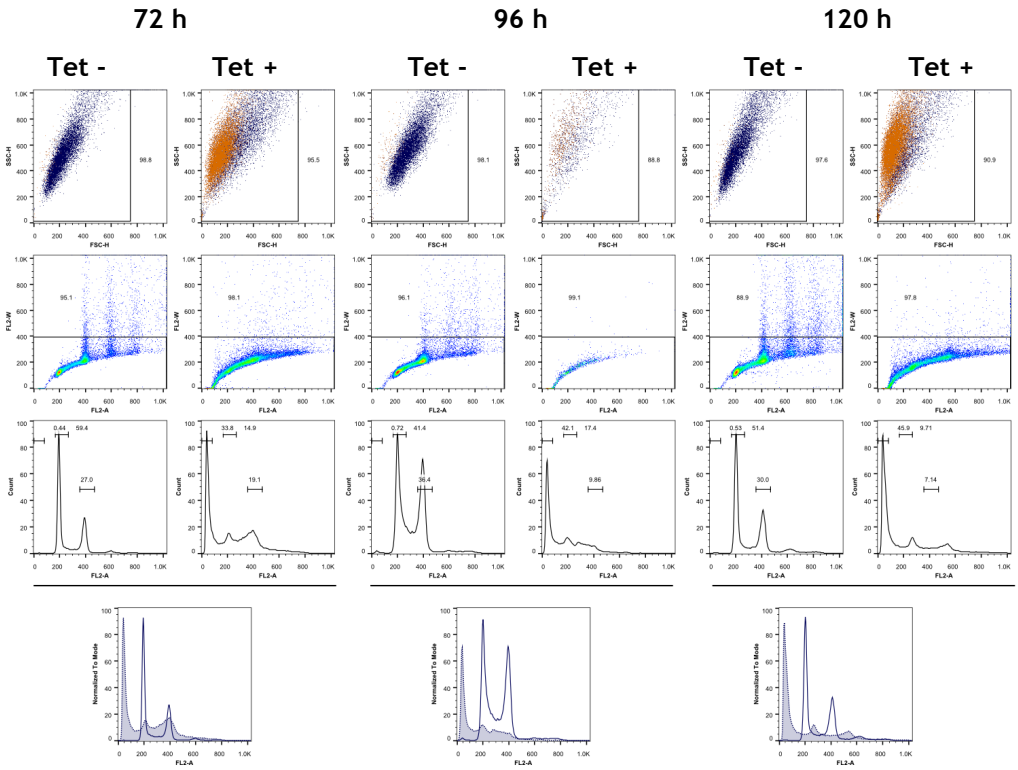

Figure 7.13. TbORC1/CDC6 RNAi Clb cell line, 72 h, 96 h and 120 h time points.
Description as in Figure 7.9.

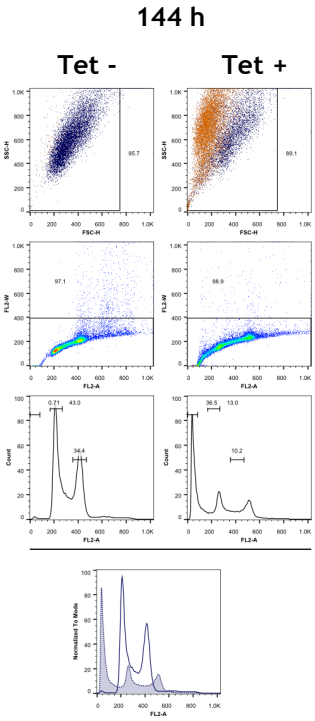

Figure 7.14. TbORC1/CDC6 RNAi Clb cell line, 144 h time points.
Description as in Figure 7.9.

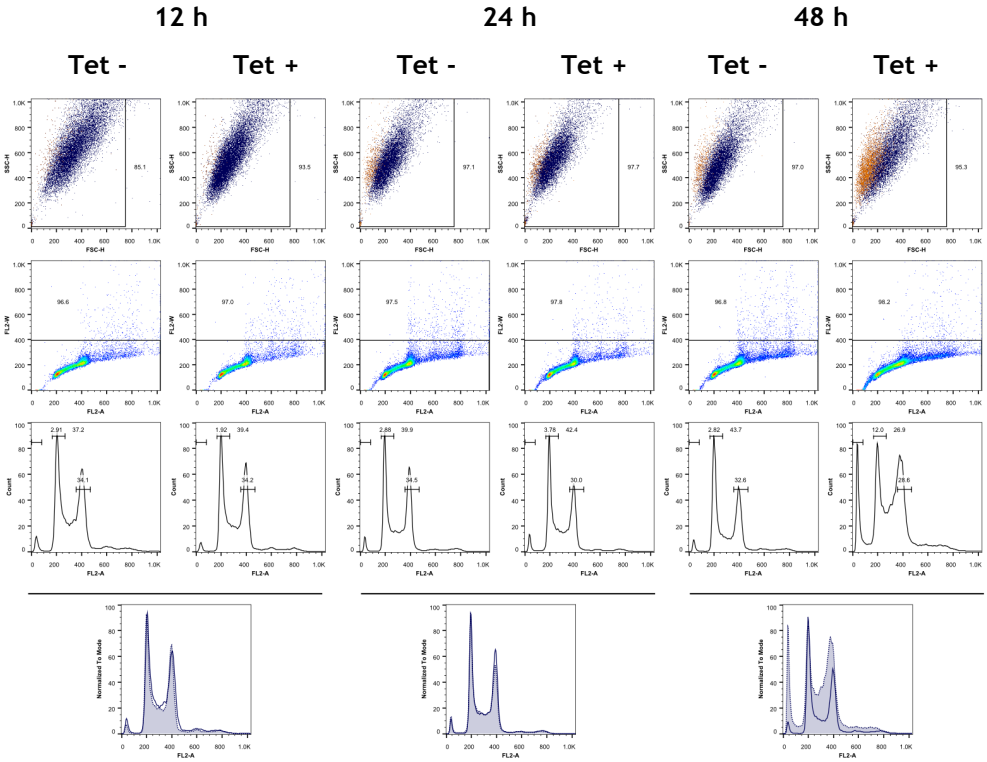

Figure 7.15. TbORC4 RNAi Cla cell line, 12 h, 24 h and 48 h time points.
Description as in Figure 7.9.

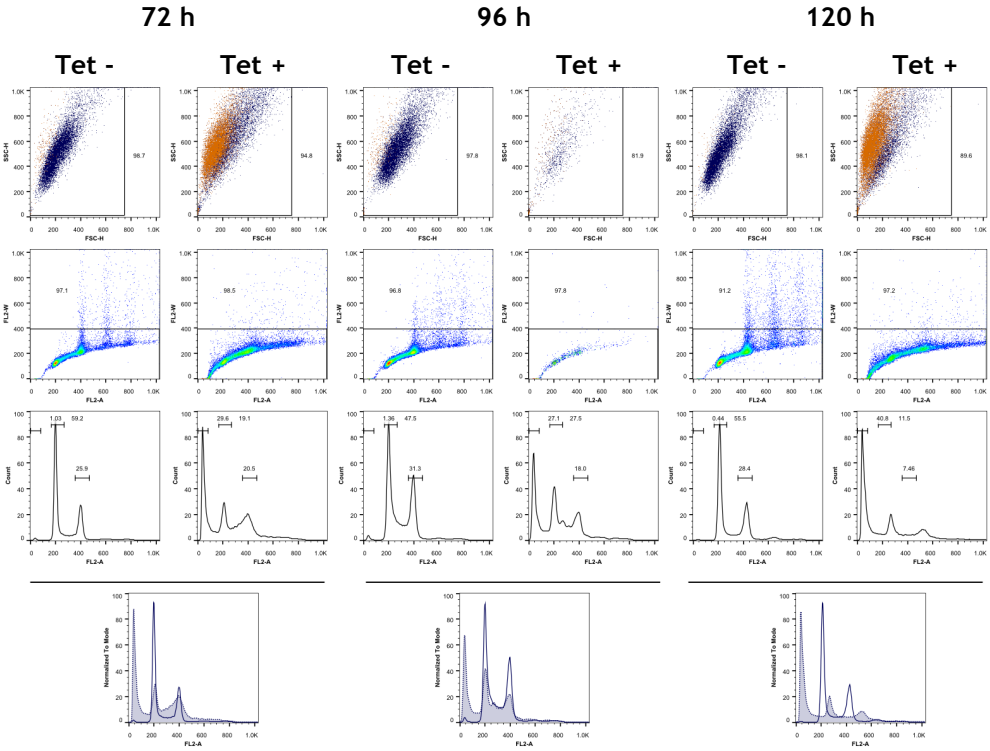

Figure 7.16. TbORC4 RNAi Cla cell line, 72 h, 96 h and 120 h time points.
Description as in Figure 7.9.

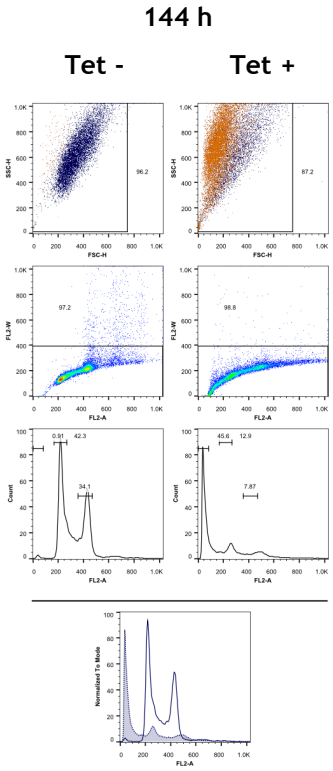

Figure 7.17. TbORC4 RNAi Cla cell line, 144 h time points.
Description as in Figure 7.9.

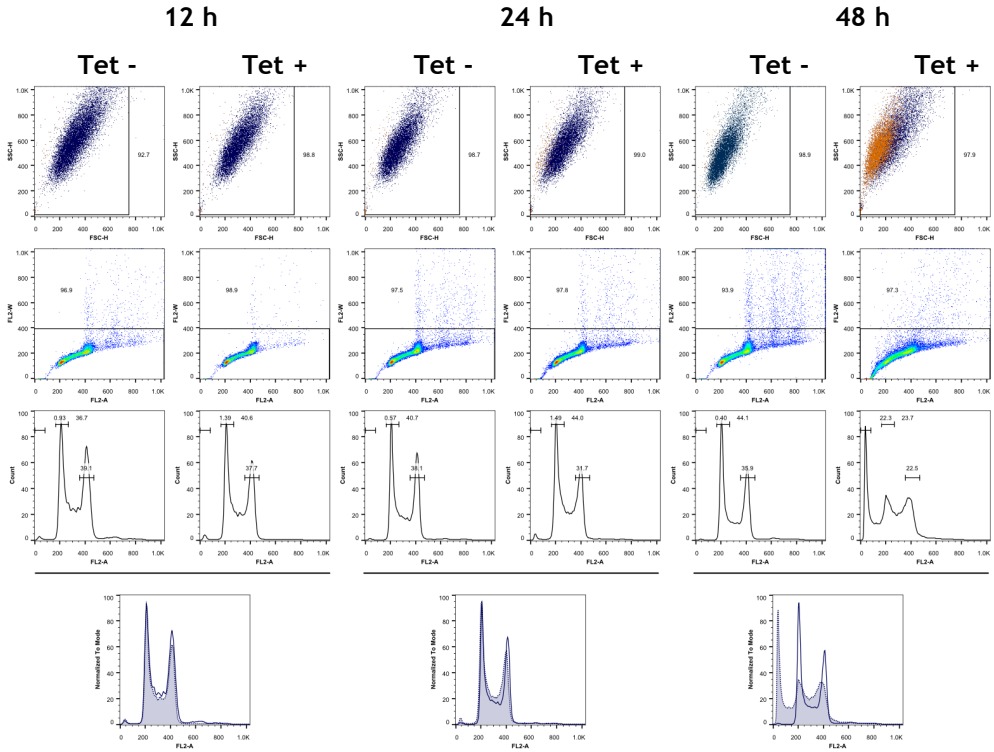

Figure 7.18. TbORC4 RNAi Clb cell line, 12 h, 24 h and 48 h time points.
Description as in Figure 7.9.

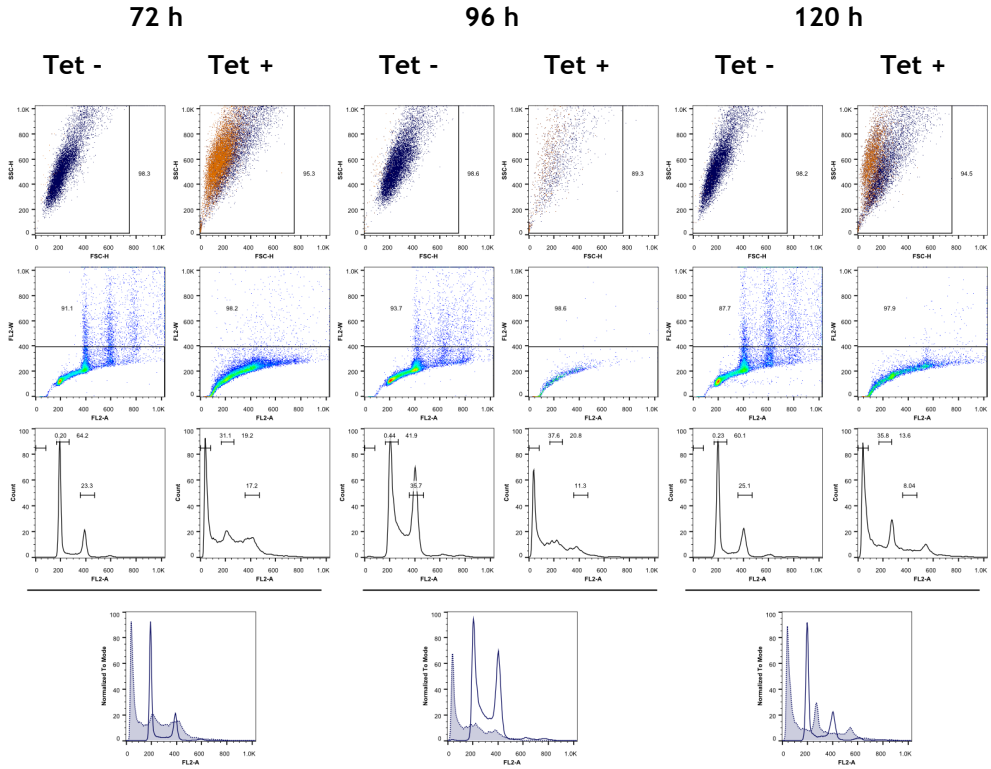

Figure 7.19. TbORC4 RNAi Clb cell line, 72 h, 96 h and 120 h time points.
Description as in Figure 7.9.

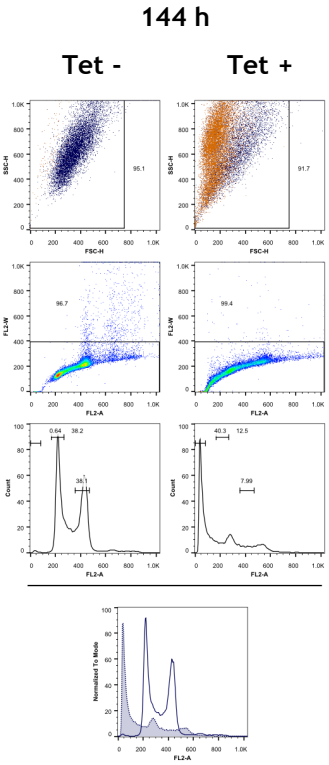

Figure 7.20. TbORC4 RNAi Clb cell line, 144 h time points.
Description as in Figure 7.9.

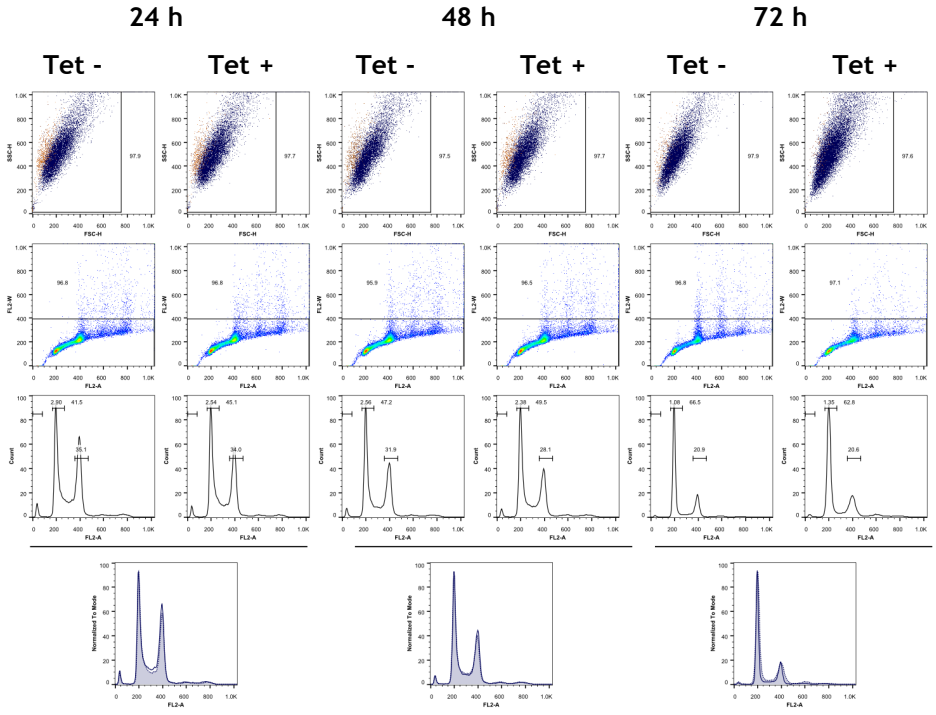

Figure 7.21. Tb3120 RNAi Clb cell line, 24 h, 48 h and 72 h time points.
Description as in Figure 7.9.

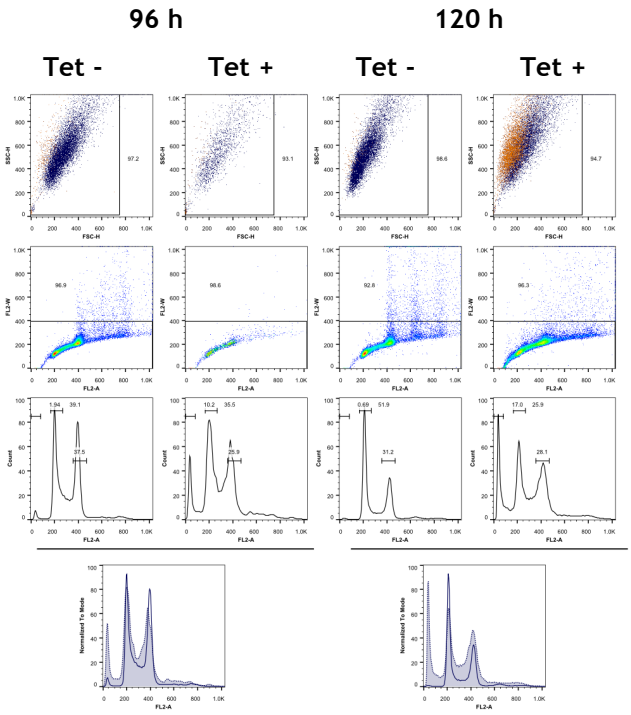

Figure 7.22. Tb3120 RNAi Clb cell line, 96 h and 120 h time points.
Description as in Figure 7.9.

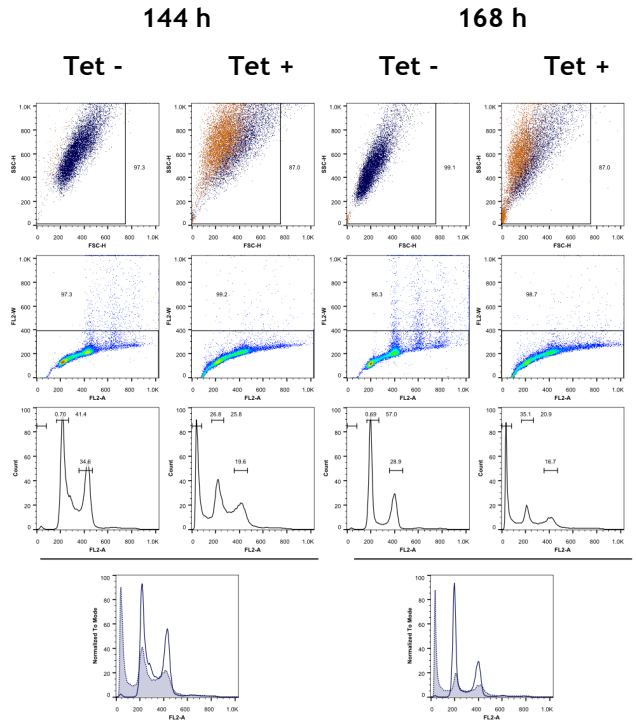

Figure 7.23. Tb3120 RNAi Clb cell line, 144 h and 168 h time points.
Description as in Figure 7.9.

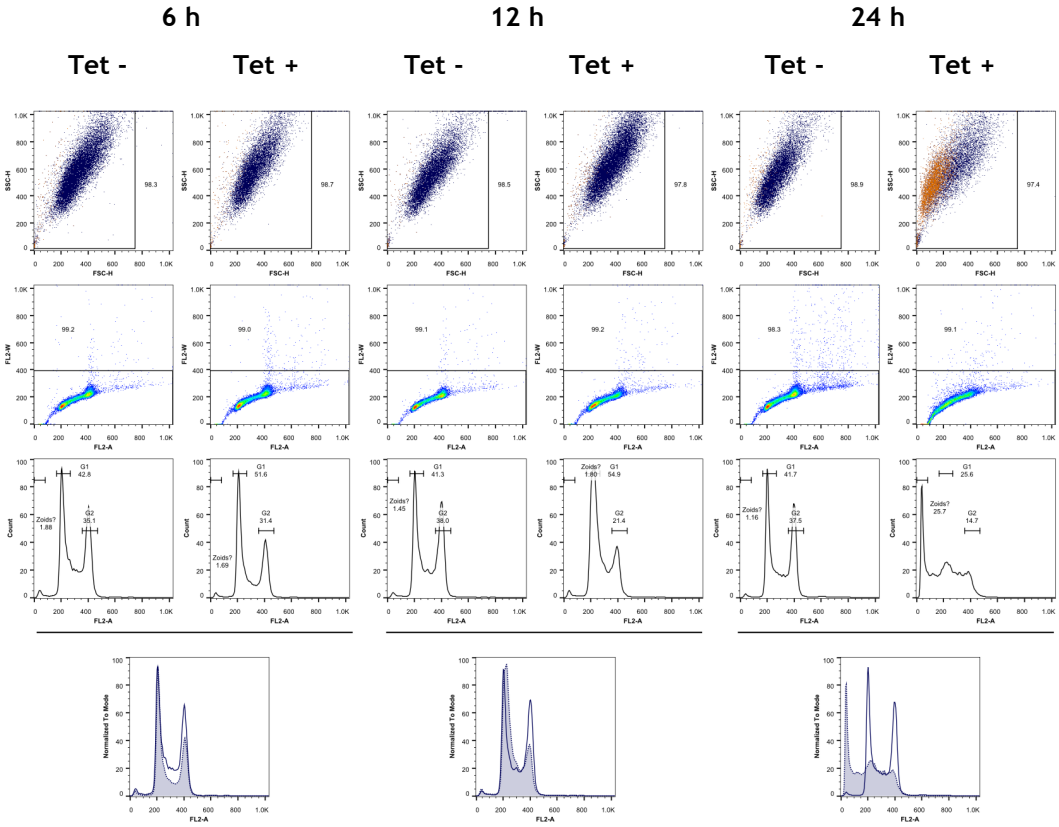

Figure 7.24. TbORC1B RNAi cell line, 6 h, 12 h and 24 h time points.
Description as in Figure 7.9.

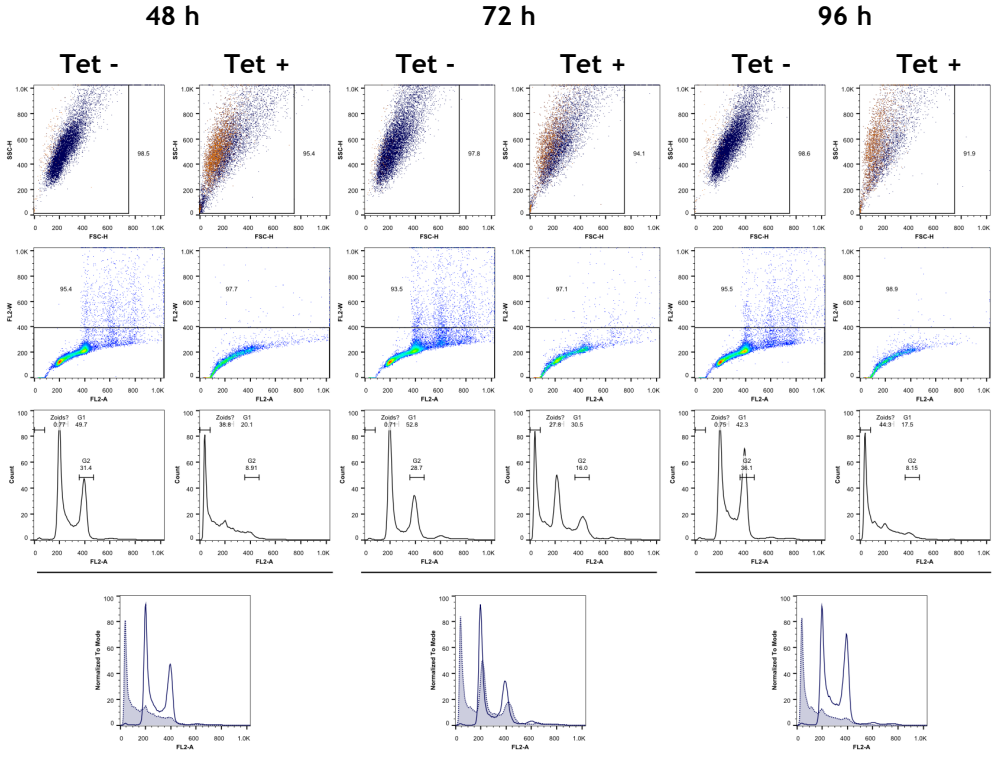

Figure 7.25. TbORC1B RNAi cell line, 48 h, 72 h and 96 h time points.
Description as in Figure 7.9.

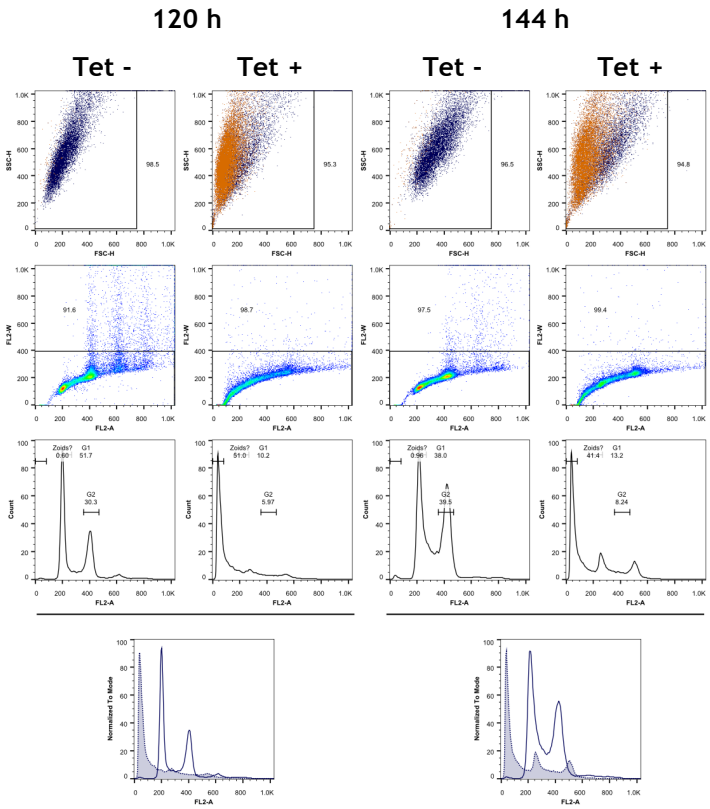

Figure 7.26. TbORC1B RNAi cell line, 120 h and 144 h time points.
Description as in Figure 7.9.

7.4 Cloning the constructs

7.4.1 Confirmation enzymatic digestion of the plasmids for endogenous tag of Lister 427 cell lines

When comparing the available sequences for the strains TREU 927 and Lister 427 of *T. brucei* (TriTrypDB, version 8.1), it was evident that there were some minor nucleotide differences between the two (Figure 7.27, Figure 7.28, Figure 7.29, Figure 7.30, Figure 7.31, and Figure 7.32). While in the case of both TbORC1/CDC6 and TbORC1B the regions used for cloning did not include any nucleotide difference that resulted in an amino acid change in the resultant proteins, the same was not observed for TbORC4, Tb7980, Tb3120 and Tb1120. To avoid any differences between strains, gDNA from TREU 927 and Lister 427 was used as a template to produce the constructs used for tagging the proteins of interest in parasites of the respective two strains. While the plasmids generated for the tagging of cells from the strain TREU 927 are shown in Chapter 3, section 3.2.1.1, the plasmids used for the tagging of cells from the Lister 427 strain are here shown in Figure 7.33.

Figure 7.27. Alignment of the DNA sequences of the TbORC1/CDC6 gene from the reference genomes of the TREU 927 and Lister 427 strains of *T. brucei*.
Only the region of the gene used for the cloning is represented. None of the nucleotide differences resulted in amino acid changes.

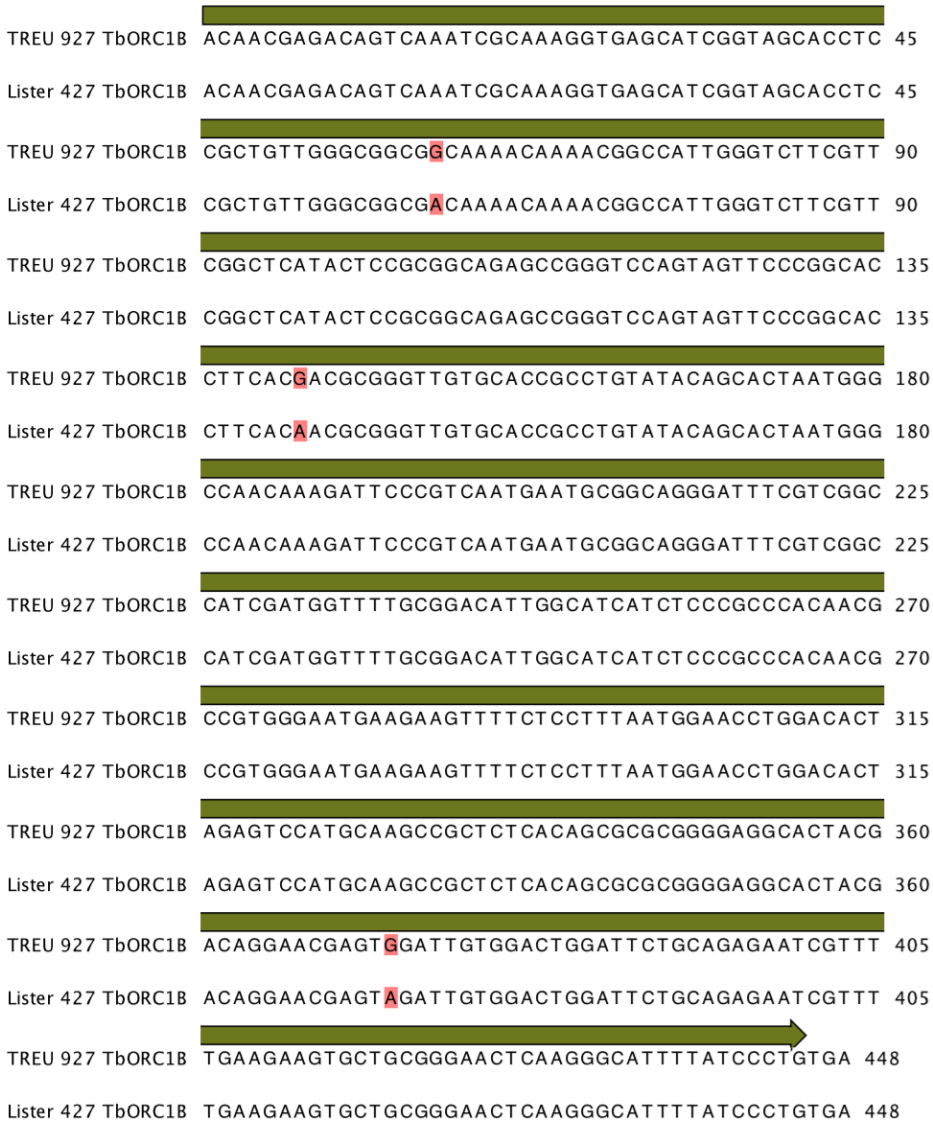

Figure 7.28. Alignment of the DNA sequences of the TbORC1B gene from the reference genomes of the TREU 927 and Lister 427 strains of *T. brucei*.
Only the region of the gene used for the cloning is represented. None of the nucleotide differences resulted in amino acid changes.

Figure 7.29. Alignment of the DNA sequences of the TbORC4 gene from the reference genomes of the TREU 927 and Lister 427 strains of *T. brucei*.
Only the region of the gene used for the cloning is represented. From the five nucleotide differences, only three result in amino acid changes.

Figure 7.30. Alignment of the DNA sequences of the Tb7980 gene from the reference genomes of the TREU 927 and Lister 427 strains of *T. brucei*.
Only the region of the gene used for the cloning is represented. Because Tb7980 was tagged in the N-terminal, both the 5' region immediately before the gene's start codon (dark red), and the first 357 bp of the gene (red), were used for cloning. Although there were no differences between the sequences of the gene, the 5' region used presented three nucleotide variances. To avoid interference with this region, plasmids were generated using gDNA from both strains.

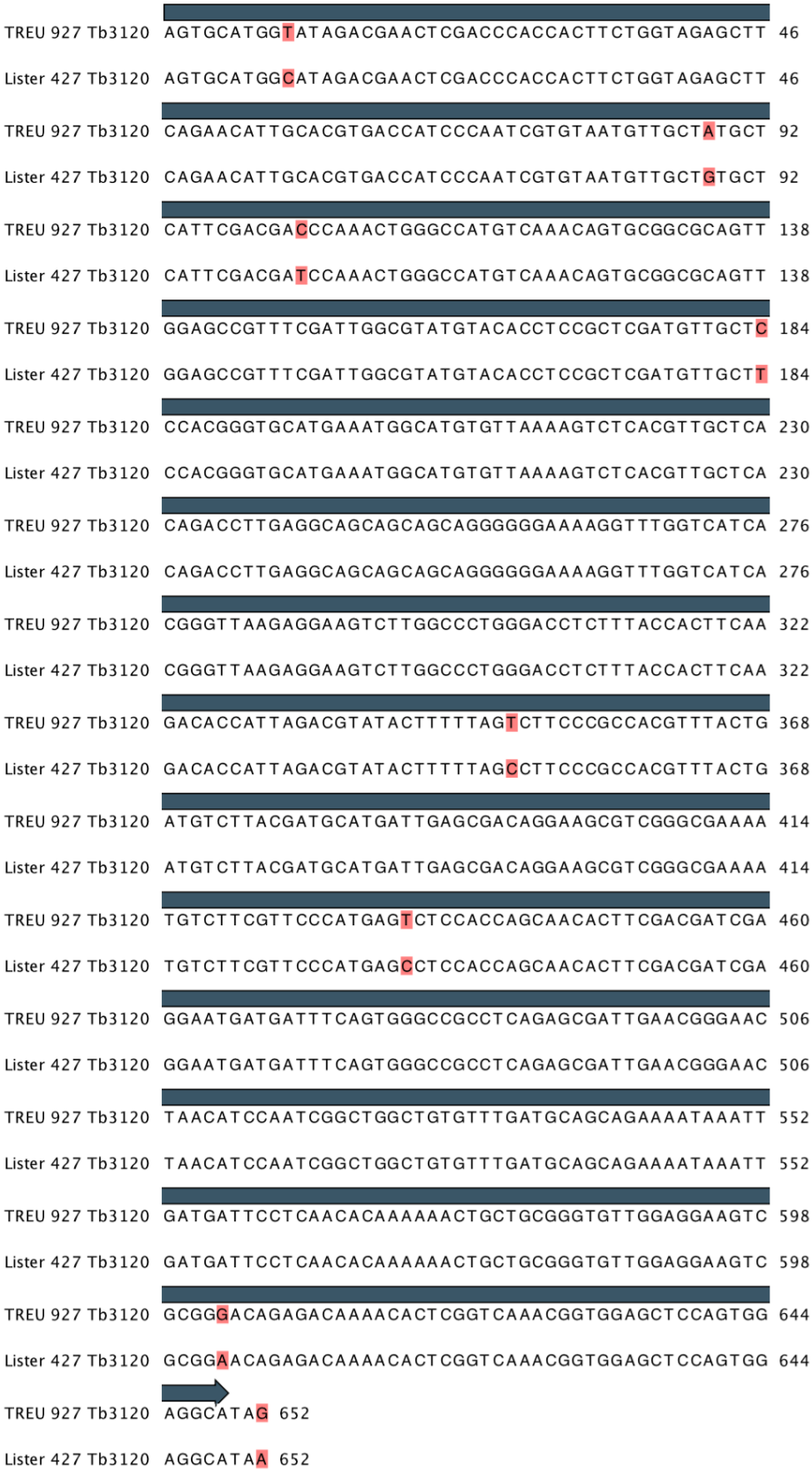

Figure 7.31. Alignment of the DNA sequences of the Tb3120 gene from the reference genomes of the TREU 927 and Lister 427 strains of *T. brucei*.
Only the region of the gene used for the cloning is represented. From the seven nucleotide differences, only one result in amino acid changes.

Figure 7.32. *(continue next page, together with description)*

Figure 7.12. Alignment of the DNA sequences of the Tb1120 gene from the available genomes of the TREU 927 and Lister 427 strains of *T. brucei*.
Only the region of the gene used for the cloning is represented. From the seven nucleotide differences, only four result in amino acid changes.

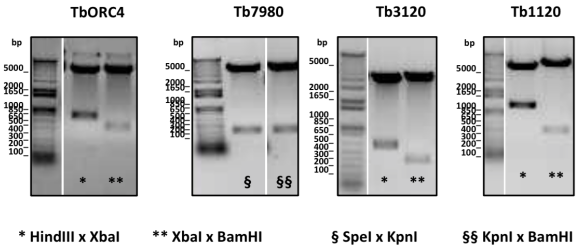

Figure 7.33. Enzymatic digestion of the plasmids used for endogenous tagging of proteins with N- or C-terminal 12-myc tag, to be used for the transfection of Lister 427 cell lines.
Description as in Chapter 3, Figure 3.13.

7.4.2 Plasmid map of the parental construct using for gene deletion

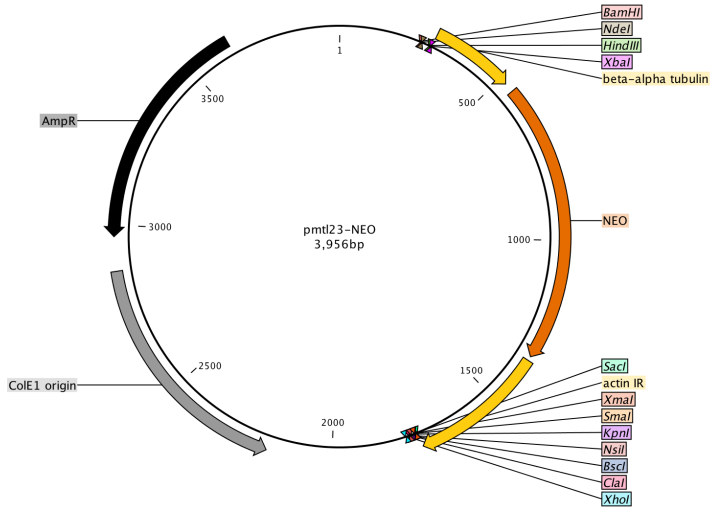

Figure 7.34. Original plasmid used for the generation of the constructs used for gene deletion described in Chapter 3.

7.5 Cell cycle mRNA levels of TbORC1/CDC6 interacting factors

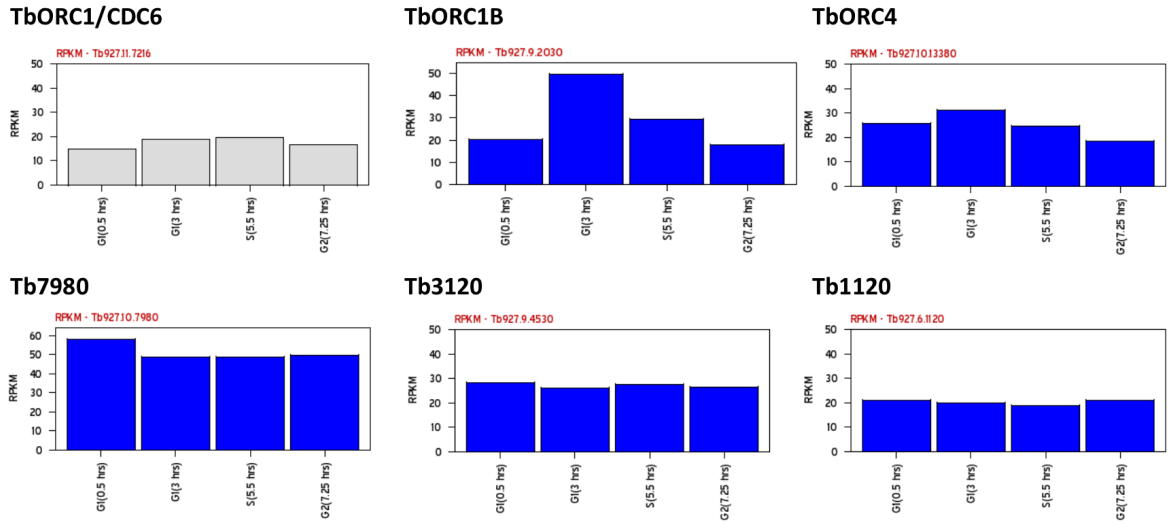

Figure 7.35. mRNA levels of TbORC1/CDC6, TbORC1B, TbORC4, Tb7980, Tb3120 and Tb1120 throughout the cell cycle.
Levels of mRNA of TbORC1/CDC6, TbORC1B, TbORC4, Tb7980, Tb3120 and Tb1120 throughout the cell cycle of PCF cells; the graphs were exported from TriTrypDB version 8.0, and represent the data originated by (Archer *et al.*, 2011).

7.6 TbORC1/CDC6 and other factors subcellular localisation

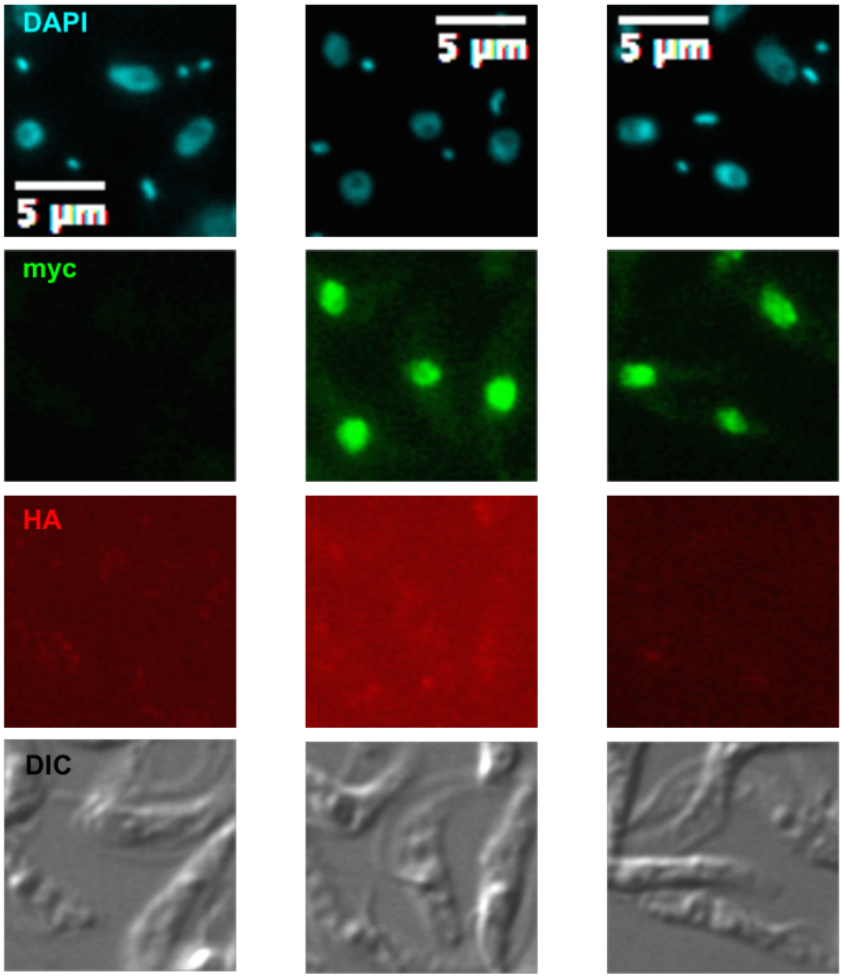

	927 wt	TbORC1/CDC6 -/12myc	TbORC1/CDC6 -/12myc TbORC1B 6HA
anti-myc	+	+	+
anti-HA	+	+	-
Anti-mouse A596	+	+	+

Figure 7.36. Immunofluorescence of TbORC1/CDC6^{12myc} and TbORC1B^{6HA}, TbORC4^{6HA}, Tb7980^{6HA}, Tb3120^{6HA}, and Tb1120^{6HA} – Controls used.
Top panel row shows the staining of the cells with DAPI. Panel row below shows detection with the anti-myc antiserum, and the next one detection with anti-HA and anti-mouse AlexaFluor® 594 conjugate antisera. Lowest panel row shows the cells outline by DIC. PCF 927 wt cells were stained for both myc and HA detection. Images show that no clear non-specific signal is detected for both tags' labelling. TbORC1/CDC6 -/12myc cells were stained for both myc and HA detection. Images show that no clear non-specific signal is detected for the HA tag detection, demonstrating that there is no interference of the signal emitted from the anti-myc antisera into the TRITC filter set (used for the detection of AlexaFluor® 594 fluorophore). TbORC1/CDC6 -/12myc TbORC1B 6HA cells were incubated with the anti-mouse AlexaFluor® 594 antiserum alone, followed by the incubation with anti-myc. Images show that the secondary antibody alone is not detecting any signal in the TRITC filter channel, and that a posterior incubation of the sample with the anti-myc antibody, raised in mouse like the anti-HA antibody, leads to no cross-detection of the myc-tagged protein.

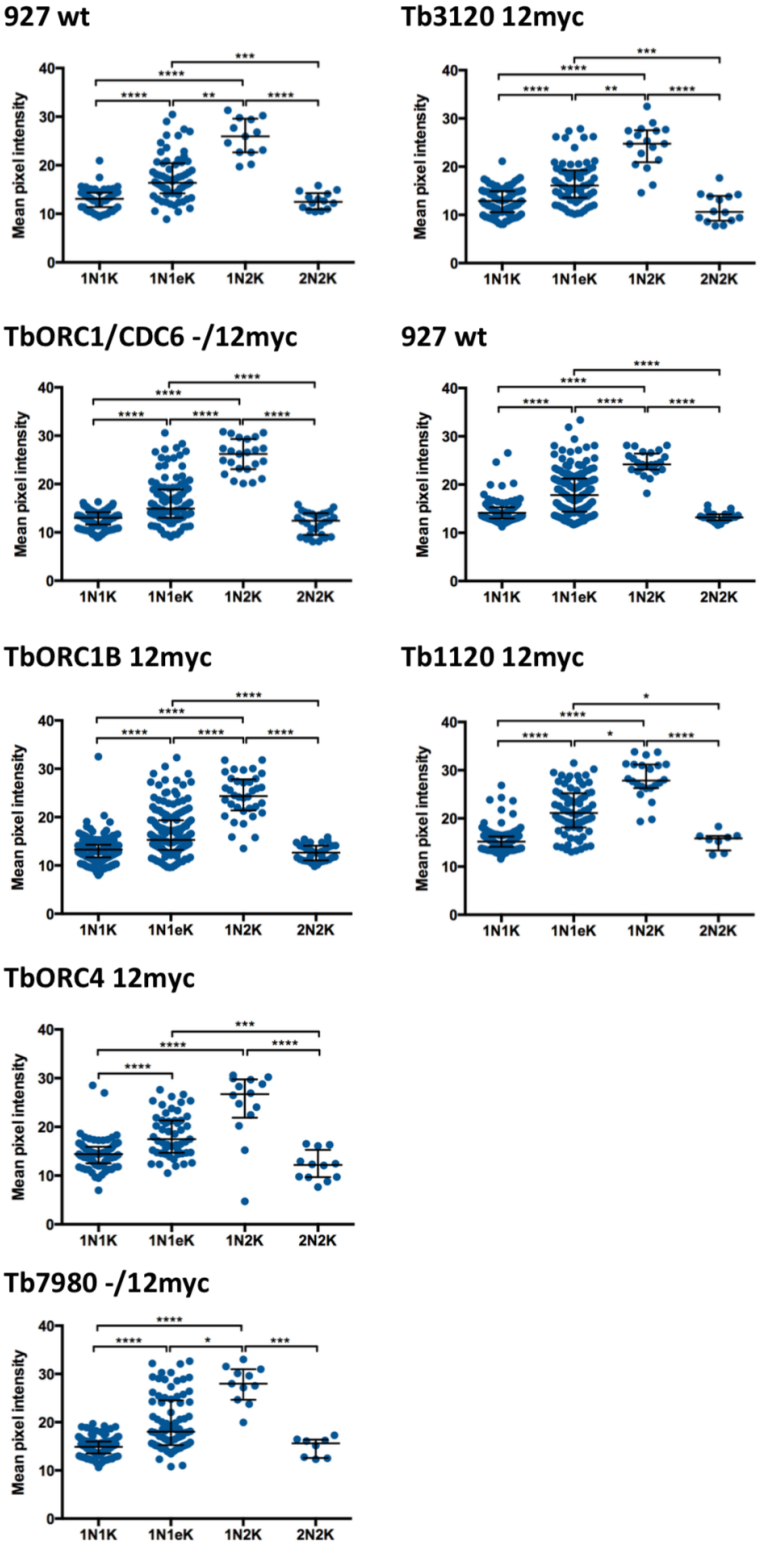

Figure 7.37. Intensity plots of DAPI signal throughout the cell cycle.
Intensity of the DAPI signal, represented (dots) as the mean of pixel intensity within the region of interest (ROI, of 21 x 21 pixels) enclosing the each cell nucleus. At least 125 cells were analysed per cell line (n ≥ 125). The median of the values is represented, with the error bars depicting the interquartile range. Statistic significance was assessed through analysis using the Kruskal-Wallis non-parametric test. (*) p-value < 0.05; (**) p-value < 0.01; (***) p-value < 0.001; (****) p-value <0.0001.

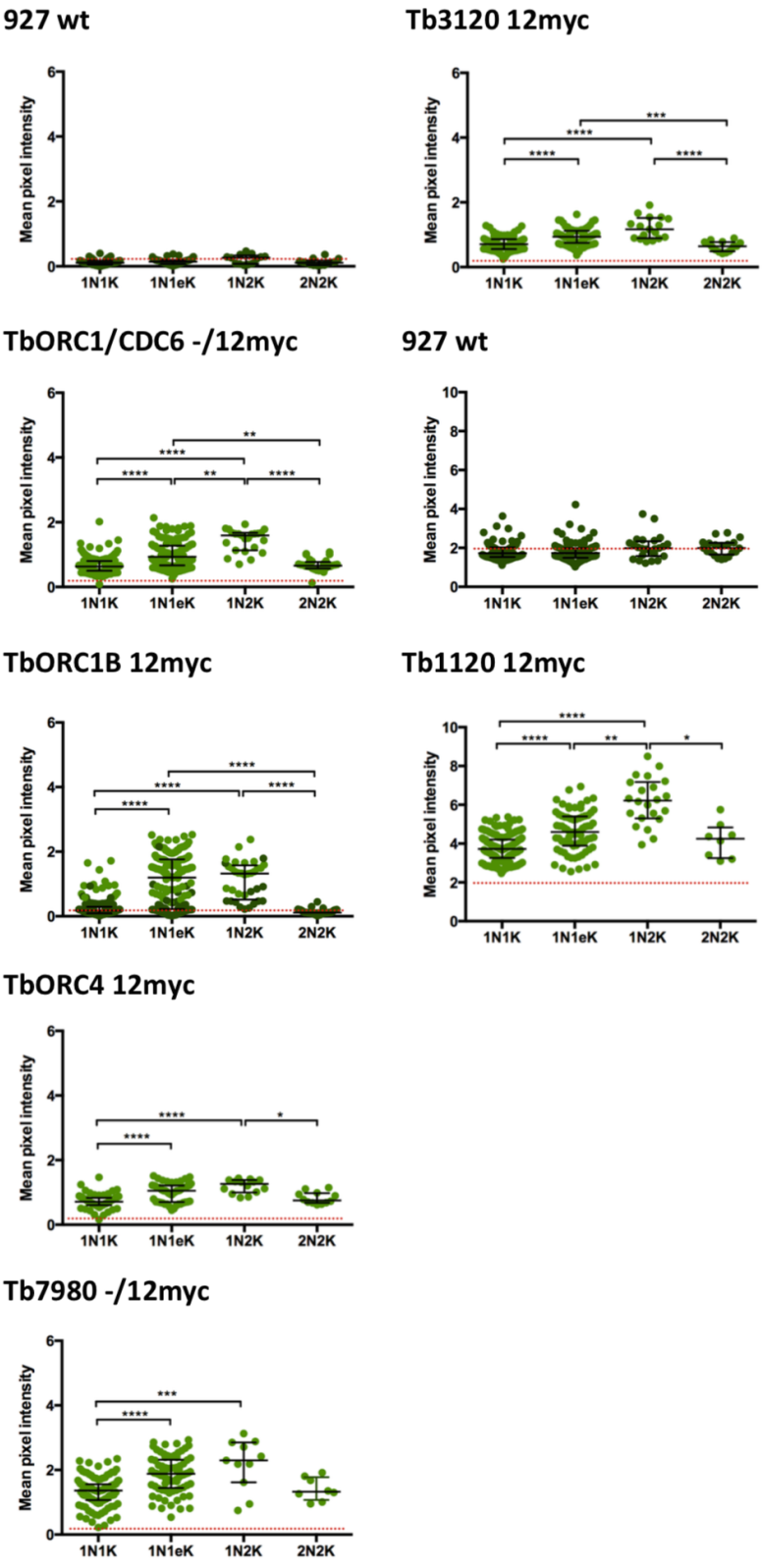

Figure 7.38. Intensity plots of myc signal throughout the cell cycle.
Intensity of the myc signal, represented (dots) as the mean of pixel intensity within the region of interest (ROI, of 21 x 21 pixels) enclosing the each cell nucleus. At least 125 cells were analysed per cell line (n ≥ 125). The median of the values is represented, with the error bars depicting the interquartile range. Statistic significance was assessed through analysis using the Kruskal-Wallis non-parametric test. (*) p-value < 0.05; (**) p-value < 0.01; (***) p-value < 0.001; (****) p-value <0.0001.

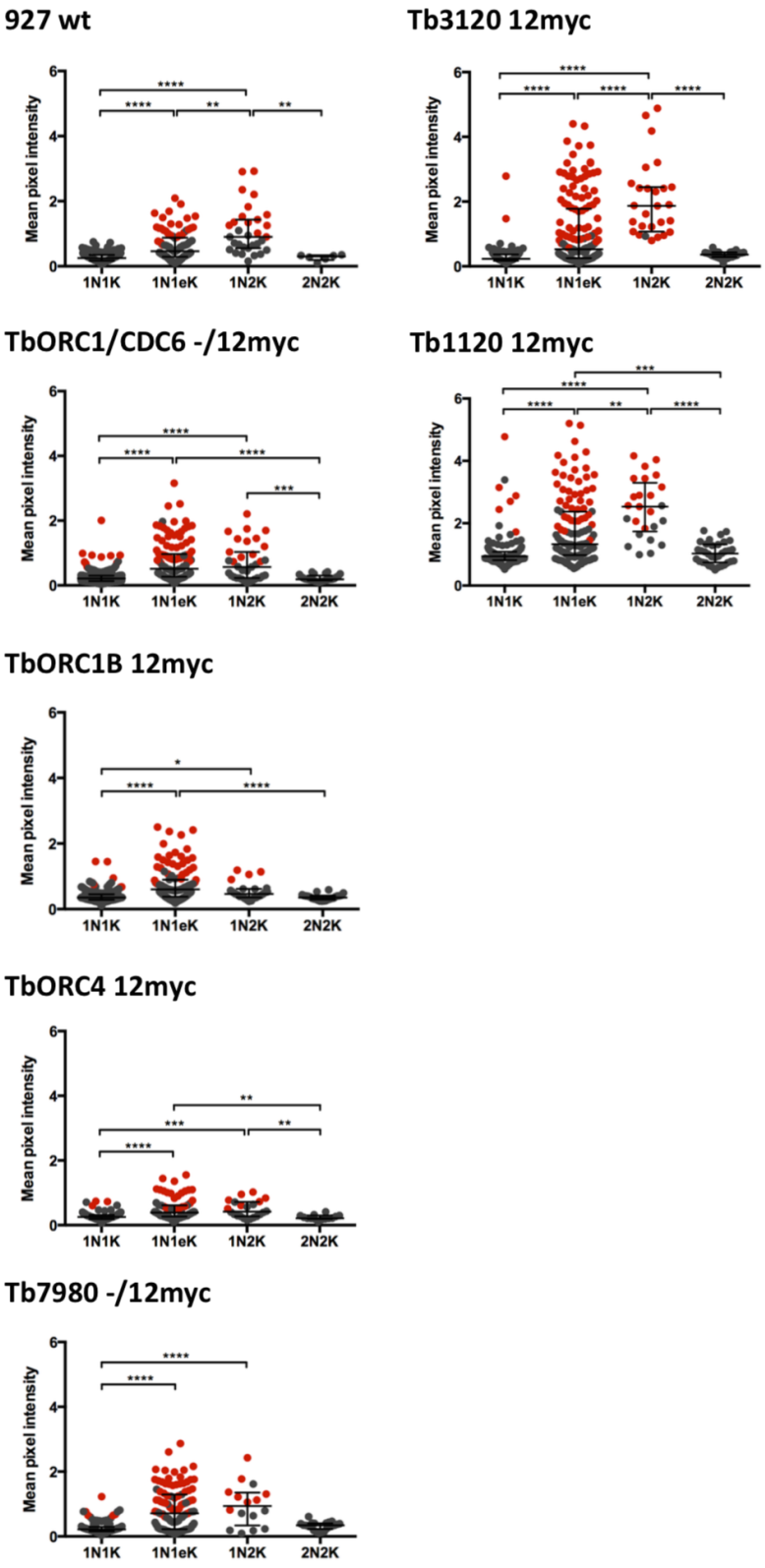

Figure 7.39. Intensity plots of EdU signal throughout the cell cycle.
Intensity of the EdU signal, represented (dots) as the mean of pixel intensity within the region of interest (ROI, of 21 x 21 pixels) enclosing the each cell nucleus. Dots in red represent cells with EdU signal with enough intensity to be perceived by eye. At least 125 cells were analysed per cell line ($n \geq 125$). The median of the values is represented, with the error bars depicting the interquartile range. Statistic significance was assessed through analysis using the Kruskal-Wallis non-parametric test. (*) p-value < 0.05; (**) p-value < 0.01; (***) p-value < 0.001; (****) p-value <0.0001.

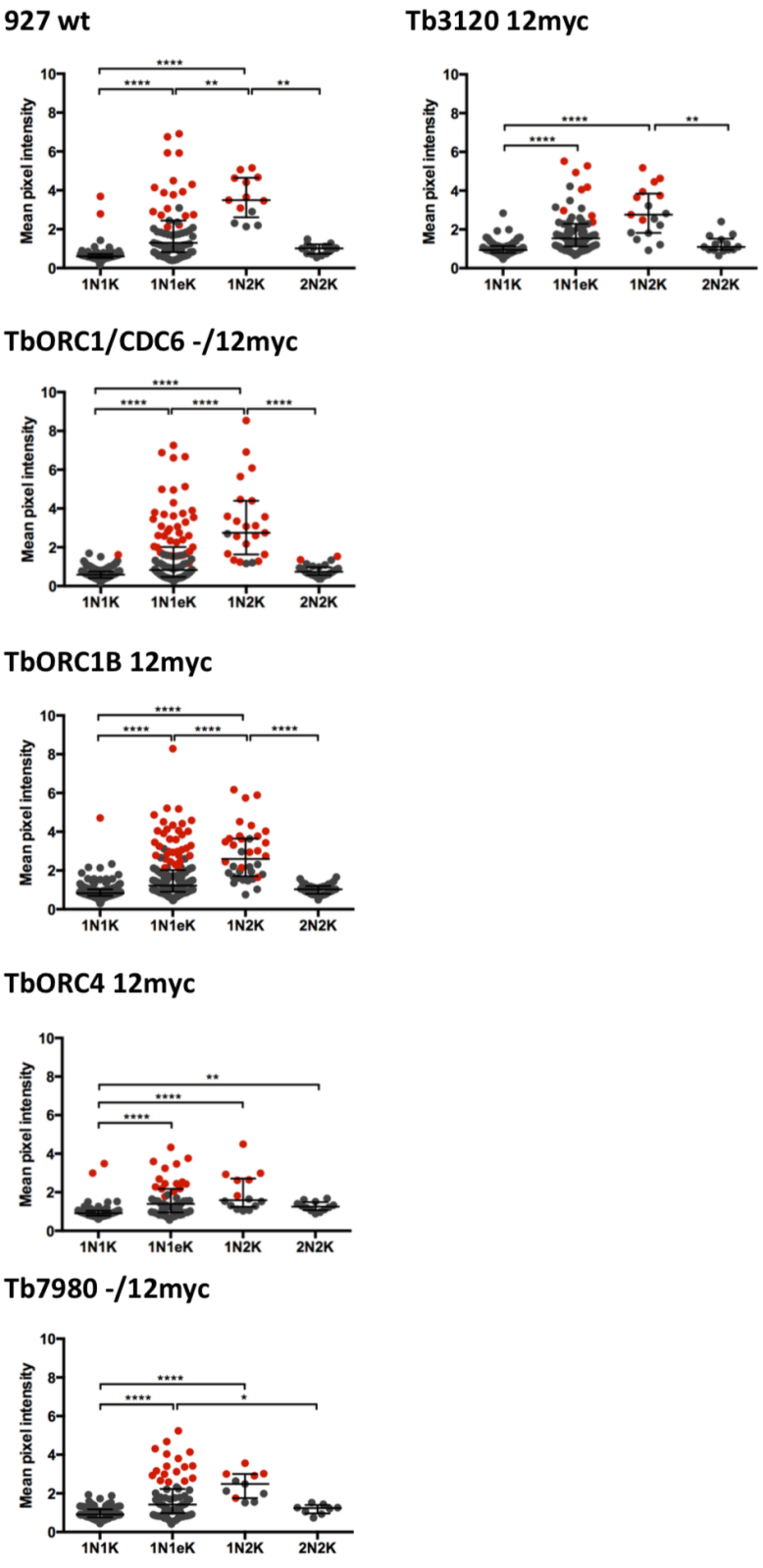

Figure 7.40. Intensity plots of EdU signal throughout the cell cycle.
Results from the experiment performed independently from the one shown in Figure 7.37 to Figure 7.39, and shown in Chapter 3 (DAPI and myc signals). Intensity of the EdU signal, represented (dots) as the mean of pixel intensity within the region of interest (ROI, of 21 x 21 pixels) enclosing the each cell nucleus. Dots in red represent cells with EdU signal with enough intensity to be perceived by eye. At least 125 cells were analysed per cell line (n ≥ 125). The median of the values is represented, with the error bars depicting the interquartile range. Statistic significance was assessed through analysis using the Kruskal-Wallis non-parametric test. (*) p-value < 0.05; (**) p-value < 0.01; (***) p-value < 0.001; (****) p-value <0.0001.

7.7 Gel Filtration of TbORC1/CDC6 12 myc

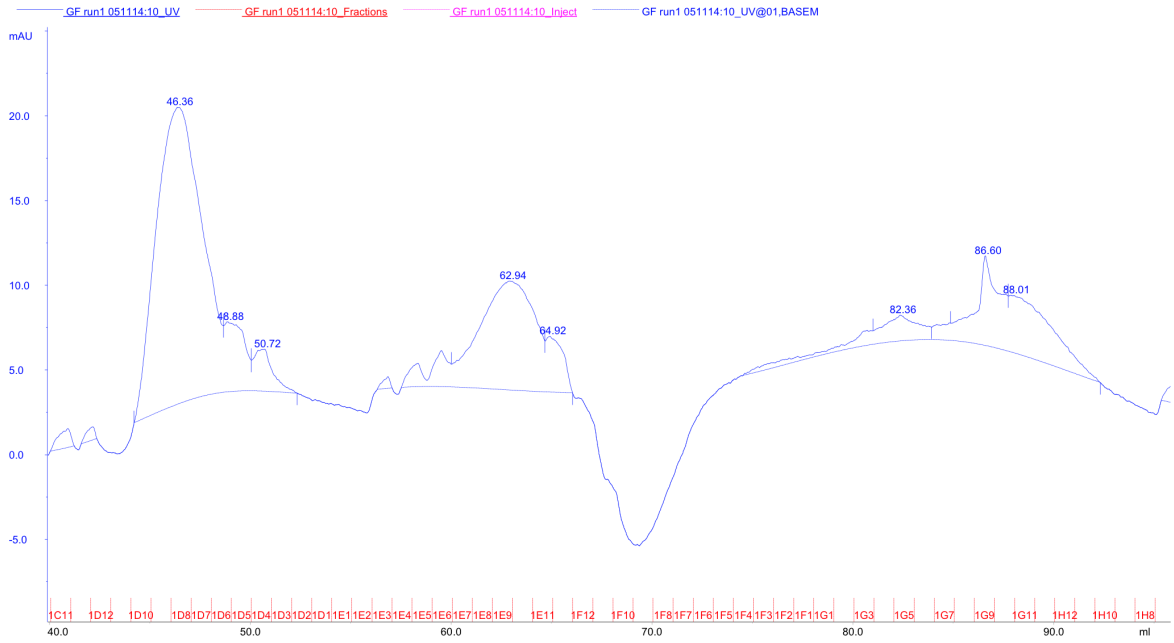

Figure 7.41. Chromatogram resultant from the gel filtration of TbORC1/CDC6 12myc. TbORC1/CDC6 -/12myc cell line was lysed and separated into fractions of 1 ml by gel filtration, which are shown in the x axis (eluted volume in ml). The red sections and numbers represent the wells in the plate in which the fraction was eluted to. The y axis represents the UV (ultraviolet) absorbance values. The samples eluted from 43 ml (1D12) to 84 ml (1G5) were selected for western blot analysis, as shown in Chapter 3, section 3.6.3.

7.8 Mapping Origins of Replication in BSF cells

The script used to map the origins of replication in BSF and PCF cells to the Lister 427 genome (Chapter 4) is shown below. The script was conceived and designed by Dr Nicholas J. Dickens, based on the methodology used previously to map the origins in PCF cells strain TREU 927 (Tiengwe *et al.*, 2012). The same script was also used to map the origins in *L. major* and *L. mexicana*, shown in Chapter 5.

```
# First step – check quality of the sequencing results
retrieved from the sequencing system. The data is obtained as
fastaq files, which are analysed using the FastQC software
package, a quality control tool for high throughput
sequencing data
(http://www.bioinformatics.babraham.ac.uk/projects/fastqc/).
This tool opens a graphical interface in which the sequences
are uploaded and analysed. The results are shown in a graphic
and quality score. A threshold was set at a quality score of
20, therefore the sequences were trimmed (below), to exclude
those poor quality reads.

# Second step – trim the reads, to exclude poor quality ones,
with a quality score lower than 20. In addition, the reads
obtained from the sequencing system contain the sequences of
the adapters used for the library preparation and sequencing
processes, and these have to be removed. For these purposes,
the fastq-mcf tool (https://code.google.com/p/ea-
utils/wiki/FastqMcf) was used.

# "dir" refers to the directory in which the files are
stored. The next line defines "dir", so that it can be later
used to call files from that specific folder using just $dir.

dir=/wtcmpdata/WTCMP/McCulloch/DNA/Trypanosoma/brucei

# -q allows to define the quality threshold, which is 20.
# -w window-size for quality trimming.
# adapters.fa refers to the file that has the adapter
sequences.
# -o output file.
# only the files for BSF early S and G2 phases are shown. All
other samples were processed identically.

fastq-mcf -q 20 -w 5 adapters.fa $dir/H9B89ADXX_BSF427-
EarleyS_GTCCGC_L001_R1_001.fastq $dir/H9B89ADXX_BSF427-
EarleyS_GTCCGC_L001_R2_001.fastq -o BSF427-earlyS-
trimmed.fwd.fastq -o BSF427-earlyS-trimmed.rev.fastq

fastq-mcf -q 20 -w 5 adapters.fa $dir/H9B89ADXX_BSF427-
G21M_TAGCTT_L001_R1_001.fastq $dir/H9B89ADXX_BSF427-
G21M_TAGCTT_L001_R2_001.fastq -o BSF427-G2-trimmed.fwd.fastq
-o BSF427-G2-trimmed.rev.fastq

# this generated the files containing the trimmed sequences.
```

```
# Third step – align the trimmed reads to the reference
genome. The reference Lister 427 genome used was retrieved
from TriTrypDB v8.0 (file name TriTrypDB-
8.0_TbruceiLister427.fa). The reference genome needs to be
indexed using the Bowtie2 v2.2.0 tool, and the reads were
aligned to the reference genome using the very sensitive
local –k1 mode.

# folder containing the reference genome file

cp /wtcmpdata/Genomes/EuPathDB/TriTrypDB-
8.0_TbruceiLister427.fa

# index of the reference genome, generating a new file
bowtie427Ref.

bowtie2-build TriTrypDB-8.0_TbruceiLister427.fa bowtie427Ref

# alignment of the BSF early S and G2 phases trimmed data to
the indexed reference genome. All other data was processed
identically.

bowtie2 -p 4 --very-sensitive-local -x bowtie427Ref -1
BSF427-earlyS-trimmed.fwd.fastq -2 BSF427-earlyS-
trimmed.rev.fastq 1> BSF427-EarlyS-aligment.sam 2> BSF427-
EarlyS-aligment.log

bowtie2 -p 4 --very-sensitive-local -x bowtie427Ref -1
BSF427-G2-trimmed.fwd.fastq -2 BSF427-G2-trimmed.rev.fastq 1>
BSF427-G2M-aligment.sam 2> BSF427-G2M-aligment.log

# Fourth step – the aligned reads are compared using a
simplified version of the method described in (Tiengwe et
al., 2012). The reads are binned in 2.5 Kbp sections along
each chromosome, and the number of reads per bin are then
used to calculate the ratios between the early S (or late S)
and G2 samples, scaled for the total size of the read library
(reads per 2.5 Kbp per million reads mapped). The output is
then used to create the graphical representations of the
chromosomes (in this case, using GraphPad, version 6.0). All
steps are done using the samtools software package.

# the bin size is set up to 2.5 Kbp

binzise=2500

# defining the reference genome to use.

refFile=/wtcmpdata/Genomes/EuPathDB/TriTrypDB-
8.0_TbruceiLister427.fa

# need to index the fasta file containing the reference
genome.

samtools faidx $refFile
```

```
# need to generate a .bed file out of the reference genome.
Use a script generated by Dr Nicholas J. Dickens. It then
bins the reference genome into 2500 bp intervals.

fai2bed="/homes/nd48m/old_Projects/2014/03_March/mfa-
seq/cfg/fai2bed.pl"

$fai2bed $refFile.fai 2500 > ref.bed

# now need to index the data files resultant from the
alignment. Again, only the BSF early S and G2 are shown, the
remaining were processed identically.

samtools index BSF427-EarlyS-aligment.sam

samtools index BSF427-G2M-aligment.sam

# the coverage of the genome with the reads from each sample
is then assessed and the output retrieved in the form of a
.bed file.

coverageBed –abam $BSF427-EarlyS-aligment.sam –b ref.bed >
BSF427vs427_EarlyS.2500.bed

coverageBed –abam $BSF427-G2M-aligment.sam –b ref.bed >
BSF427vs427_G2M.2500.bed

# the ratios between the coverage of the early S (or late S)
phase and G2 phase samples are calculated.

# for simplicity, labels are given to the bed files.

bed1=BSF427vs427_EarlyS.2500.bed

bed2=BSF427vs427_G2M.2500.bed

# output file with the final results to then be used to
create the graphs.

out=2040816_BSF427vs427_EarlyS_v_g2.2500.bedgraph

# get the total number of aligned reads for each bam file

total1=`awk 'BEGIN{sum=0}{ sum+=$4} END {print sum}' $bed1`

total2=`awk 'BEGIN{sum=0}{ sum+=$4} END {print sum}' $bed2`


# create a bedgraph of the files

paste $bed1 $bed2 | awk 'BEGIN{FS="\t";
OFS="\t";scale='$total2'/'$total1'}{if($11==0){next;}}{print
$1,$2,$3,scale * $4/$11}' > $out
```

7.9 Origin and non-origins size in *T. brucei*, *L. major*, and *L. mexicana*

Table 7-1. *T. brucei* distance in Kbp between the first two genes within the SSRs, with or no origin activity detected by MFA-seq..

	Origins				Non-origins			
Chr	Gene left	Gene right	SSR type	origin (kb)	Gene left	Gene right	SSR type	non-origin
1	unclear, it's at the centromere				Tb927.1.2080	Tb927.1.200	dss	5.068
2	Tb927.2.5710	Tb927.2.5720	h-t	1.047	Tb927.2.2590	Tb927.2.2650	dss	8.063
	Tb927.2.1600	Tb927.2.1680	dss	7.987	Tb927.2.5080	Tb927.2.5120	dss	6.795
					Tb927.2.3330	Tb927.2.3340	css	1.377
					Tb927.2.5360	Tb927.2.5410	css	6.485
3	unclear, it's at the centromere				Tb927.3.580	Tb927.3.590	dss	18.339
	Tb927.3.4390	Tb927.3.4400	h-t	10.145	Tb927.3.860	Tb927.3.860	dss	4.247
					Tb927.3.1030	Tb927.3.1040	h-t	4.965
					Tb927.3.2260	Tb927.3.2270	dss	2.434
					Tb927.3.4890	Tb927.3.4900	dss	2.447
4	Tb927.4.1190	Tb927.4.1210	h-t	11.082	Tb927.4.2080	Tb927.4.2090	dss	5.132
	Tb927.4.3740	Tb927.4.3760	h-t	36.352	Tb927.4.5390	Tb927.4.5400	dss	10.255
	Tb927.4.4660	Tb927.4.4670	h-t	8.668	Tb927.4.5080	Tb927.4.5090	h-t	1.899
5	unclear, it's at the centromere				Tb927.5.1580	Tb927.5.1590	dss	6.642
	Tb927.5.2150	Tb927.5.2160	dss	10.705	Tb927.5.2900	Tb927.5.2910	dss	6.688
	Tb927.5.4530	Tb927.5.4540	dss	8.14	Tb927.5.3500	Tb927.5.3510	dss	2.199
6	unclear, it's at the centromere				Tb927.6.750	Tb927.6.760	dss	5.965
	Tb927.6.4580	Tb927.6.4590	dss	7.145	Tb927.6.1290	Tb927.6.1300	h-t	9.803
					Tb927.6.2150	Tb927.6.2160	dss	4.216
7	unclear, it's at the centromere				Tb927.6.5200	Tb927.6.5210	css	4.774
	Tb927.7.920	Tb927.7.930	dss	7.236	Tb927.7.1360	Tb927.7.1370	h-t	3.452
					Tb927.7.1940	Tb927.7.1950	css	1.154
					Tb927.7.2730	Tb927.7.2740	dss	5.79
					Tb927.7.3470	Tb927.7.3480	h-t	3.65
					Tb927.7.3880	Tb927.7.3890	dss	5.56
8	Tb927.8.1370	Tb927.8.1380	dss	0.414	Tb927.8.1940	Tb927.8.1950	dss	2.414
	Tb927.8.2880	Tb927.8.2890	dss	1.076	Tb927.8.1650	Tb927.8.1970	css	8.651
	Tb927.8.3930	Tb927.8.3940	h-t	4.781	Tb927.8.3520	Tb927.8.3530	css	6.603
	Tb927.8.4890	Tb927.8.4900	dss	7.252	Tb927.8.4760	Tb927.8.4770	h-t	5.271
	Tb927.8.6560	Tb927.8.6570	css	6.468	Tb927.8.5430	Tb927.8.5440	dss	4.763
	Tb927.8.7740	Tb927.8.7750	h-t	12.05	Tb927.8.5920	Tb927.8.5930	h-t	0.922
					Tb927.8.6920	Tb927.8.6930	dss	4.422
9	Tb927.9.3130	Tb927.9.3180	dss	4.10	Tb927.9.1960	Tb927.9.1970	h-t	5.87
	Tb927.9.7280	Tb927.9.7290	css	2.59	Tb927.9.4900	Tb927.9.4910	h-t	0.54
	Tb927.9.11150	Tb927.9.11220	dss	6.33	Tb927.9.9870	Tb927.9.9940	h-t	5.41
	Tb927.9.14510	Tb927.9.14530	dss	3.54	Tb927.9.8880	Tb927.9.8950	h-t	9.64
					Tb927.9.13150	Tb927.9.13160	css	2.12
10	Tb927.9.3040	Tb927.10.3060	h-t	4.06	Tb927.10.2450	Tb927.10.2460	dss	1.36
	Tb927.10.4960	Tb927.10.4970	dss	4.77	Tb927.10.4180	Tb927.10.4190	dss	3.34
	Tb927.10.6420	Tb927.10.6430	dss	5.40	Tb927.10.8340	Tb927.10.8350	dss	2.64
	Tb927.10.7630	Tb927.10.7640	dss	0.57	Tb927.10.11270	Tb927.10.11280	dss	4.30
	Tb927.10.9670	Tb927.10.9590	h-t	1.86	Tb927.10.12550	Tb927.10.12570	h-t	3.49
	Tb927.10.10850	Tb927.10.10870	h-t	12.03	Tb927.10.13550	Tb927.10.13560	h-t	5.25
					Tb927.10.14000	Tb927.10.14010	h-t	1.39
					Tb927.10.14840	Tb927.10.14860	dss	8.65

Table 7-1. *(continue).*

	Origins				Non-origins			
Chr	Gene left	Gene right	SSR type	origin (kb)	Gene left	Gene right	SSR type	non-origin
11	Tb927.10.720	Tb927.10.730	dss	6.24	Tb927.11.3220	Tb927.11.3230	dss	8.53
	Tb927.11.1920	Tb927.11.1930	dss	5.11	Tb927.11.3560	Tb927.11.3570	h-t	4.51
	Tb927.11.4760	Tb927.11.4780	h-t	10.25	Tb927.11.6300	Tb927.11.6310	h-t	0.13
	Tb927.11.6720	Tb927.11.6730	h-t	1.01	Tb927.11.7213	Tb927.11.7214	dss	4.85
	Tb927.11.7970	Tb927.11.7980	dss	1.93	Tb927.11.8840	Tb927.11.20730	h-t	9.28
	Tb927.11.9810	Tb927.11.9820	dss	7.06	Tb927.11.11400	Tb927.11.11420	h-t	6.38
	Tb927.11.11060	Tb927.11.11080	h-t	8.90	Tb927.11.11980	Tb927.11.12020	h-t	5.80
					Tb927.11.13710	Tb927.11.13720	dss	2.23
					Tb927.11.15380	Tb927.11.15390	h-t	5.897
					Tb927.11.16170	Tb927.11.16180	dss	3.941
					Tb927.11.6250	Tb927.11.14630	css	1.873
					Tb927.11.12710	Tb927.11.12720	css	1.389
					Tb927.11.5920	Tb927.11.5940	css	2.749
					Tb927.11.4120	Tb927.11.4130	css	1.598
					Tb927.11.2400	Tb927.11.2410	css	11.902

Table 7-2. *L. major* distance in Kbp between the first two genes within the SSRs, with or no origin activity detected by MFA-seq.

	Origins				Non-origins			
Chr	Gene left	Gene right	SSR type	origin (kb)	Gene left	Gene right	SSR type	non-origin
1	unclear				LmjF.01.0315	LmjF.01.0320	dss	0.973
2	LmjF.02.0570	LmjF.02.SLRNA.0010	dss	8.342	unclear			
3	LmjF.03.0670	LmjF.03.0690	css	13.304	LmjF.03.0010	LmjF.03.0020	dss	1.296
					LmjF.03.0970	LmjF.03.0980	h-t	0.683
4	LmjF.04.0380	LmjF.04.0390	css	9.03	LmjF.04.0625	LmjF.04.0630	h-t	0.678
5	LmjF.05.1040	LmjF.05.1050	dss	1.453	LmjF.05.0450	LmjF.05.0460	h-t	0.893
6	LmjF.06.0360	LmjF.06.0370	dss	5.747	LmjF.06.0560	LmjF.06.0570	h-t	1.351
					LmjF.06.1250	LmjF.06.1260	css	2.786
					LmjF.06.1290	LmjF.06.1300	dss	4.79
7	LmjF.07.0470	LmjF.07.0475	dss	7.646	LmjF.07.0010	LmjF.07.0020	dss	5.105
					LmjF.07.0802	LmjF.07.0805	h-t	1.032
8	LmjF.08.1090	LmjF.08.1101	dss	11.792	LmjF.08.0860	LmjF.08.0870	css	3.724
9	LmjF.09.0690	LmjF.09.0700	css	6.475	LmjF.09.1000	LmjF.09.1010	dss	3.464
10	LmjF.10.0600	LmjF.10.0610	h-t	6.454	LmjF.10.1227	LmjF.10.1228	dss	1.189
					LmjF.10.0030	LmjF.10.0040	dss	9.307
					LmjF.10.0510	LmjF.10.0520	css	4.084
11	LmjF.11.0475	LmjF.11.0480	h-t	9.055	LmjF.11.0920	LmjF.11.0930	h-t	3.031
12	LmjF.12.0510	LmjF.12.0520	dss	10.541	LmjF.12.0400	LmjF.12.0405	css	2.353
					LmjF.12.0010	LmjF.12.0020	h-t	0.416
13	LmjF.13.0450	LmjF.13.0460	dss	5.679	LmjF.13.0700	LmjF.13.0710	css	1.286
					LmjF.13.1370	LmjF.13.1380	h-t	1.025
					LmjF.13.1680	LmjF.13.1690	dss	1.847
14	LmjF.14.0470	LmjF.14.0480	css	9.477	LmjF.14.1050	LmjF.14.1060	dss	2.186
15	LmjF.15.0740	LmjF.15.0750	css	8.166	LmjF.15.0223	LmjF.15.0225	dss	1.054
					LmjF.15.1560	LmjF.15.1570	dss	4.443
16	LmjF.16.0920	LmjF.16.0930	dss	5.697	LmjF.16.1130	LmjF.16.1140	css	0.949
					LmjF.16.1520	LmjF.16.1530	dss	2.923
17	LmjF.17.0733	LmjF.17.0790	h-t	6.894	LmjF.17.0860	LmjF.17.0870	dss	1.637
					LmjF.17.0340	LmjF.17.0350	h-t	2.032
18	LmjF.18.1050	LmjF.18.1060	h-t	6.521	LmjF.18.0560	LmjF.18.0570	dss	1.826
19	LmjF.19.1420	LmjF.19.1430	h-t	9.272	LmjF.19.0980	LmjF.19.0985	h-t	5.121
					LmjF.19.0220	LmjF.19.0230	dss	7.524

Table 7-2. *(continue).*

	Origins				Non-origins			
Chr	Gene left	Gene right	SSR type	origin (kb)	Gene left	Gene right	SSR type	non-origin
20	LmjF.20.1175	LmjF.20.1180	h-t	7.807	LmjF.20.0840	LmjF.20.0850	h-t	0.715
					LmjF.20.0260	LmjF.20.0625	dss	1.32
					LmjF.20.1450	LmjF.20.1460	css	1.498
21	LmjF.21.0720	LmjF.21.0725	dss	7.465	LmjF.21.0015	LmjF.21.0020	dss	0.92
					LmjF.21.0520	LmjF.21.0530	css	1.824
					LmjF.21.1090	LmjF.21.1100	css	1.665
					LmjF.21.1720	LmjF.21.1730	dss	1.603
22	LmjF.22.1480	LmjF.22.1490	dss	6.176	LmjF.22.0790	LmjF.22.0800	dss	1.73
					LmjF.22.1220	LmjF.22.1230	css	0.938
					LmjF.22.0010	LmjF.22.0020	h-t	5.944
23	LmjF.23.1155	LmjF.23.1160	dss	5.259	LmjF.23.1630	LmjF.23.1640	css	3.237
					LmjF.23.0010	LmjF.23.0020	h-t	1.736
24	LmjF.24.1300	LmjF.24.1310	h-t	4.69	LmjF.24.0650	LmjF.24.0660	h-t	1.012
					LmjF.24.1900	LmjF.24.1905	h-t	0.518
					LmjF.24.2330	LmjF.24.2340	dss	1.239
					LmjF.24.1640	LmjF.24.1650	css	4.483
					LmjF.24.0010	LmjF.24.0020	h-t	0.683
25	LmjF.25.1460	LmjF.25.1470	h-t	1.216	LmjF.25.0715	LmjF.25.0720	dss	2.555
					LmjF.25.1080	LmjF.25.1090	css	2.532
					LmjF.25.2160	LmjF.25.2170	dss	1.363
26	LmjF.26.1665	LmjF.26.1670	h-t	5.82	LmjF.26.1015	LmjF.26.1020	dss	1.475
					LmjF.26.0760	LmjF.26.0770	h-t	0.811
					LmjF.26.2270	LmjF.26.2280	h-t	1.734
27	LmjF.27.2337	LmjF.27.rRNA.01	dss	7.629	LmjF.27.1265	LmjF.27.1270	dss	1.816
					LmjF.27.0290	LmjF.27.0300	dss	3.636
28	LmjF.28.2100	LmjF.28.2110	dss	4.37	LmjF.28.0770	LmjF.28.0785	dss	1.091
					LmjF.28.0350	LmjF.28.0360	css	0.622
					LmjF.28.1570	LmjF.28.1580	css	8.18
					LmjF.28.2690	LmjF.28.2700	css	0.656
29	LmjF.29.0885	LmjF.29.0890	dss	6.134	LmjF29.1800	LmjF.29.1810	h-t	2.489
					LmjF.29.2350	LmjF.29.2360	dss	1.331
					LmjF.29.1440	LmjF.29.1450	css	5.27
30	LmjF.30.0710	LmjF.30.0720	dss	5.046	LmjF.30.1730	LmjF.30.1740	h-t	0.84
					LmjF.30.2090	LmjF.30.2100	css	0.938
					LmjF.30.3235	LmjF.30.3240	dss	3.884
31	LmjF.31.1640	LmjF.31.1650	h-t	5.505	LmjF.31.0570	LmjF.31.0580	h-t	4.409
					LmjF.31.1230	LmjF.31.1240	h-t	3.127
					LmjF.31.1990	LmjF.31.2000	h-t	6.972
					LmjF.31.2715	LmjF.31.2720	h-t	1.024
					LmjF.31.3160	LmjF.31.3170	dss	1.679
32	LmjF.32.2985	LmjF.32.2990	dss	7.068	LmjF.32.2155	LmjF.32.2160	h-t	1.434
					LmjF.32.1370	LmjF.32.1380	css	4.191
					LmjF.32.0480	LmjF.32.0490	dss	1.907
33	LmjF.33.1610	LmjF.33.1620	h-t	6.358	LmjF.33.1790	LmjF.33.1800	dss	1.163
					LmjF.33.0600	LmjF.33.0605	dss	3.006
					LmjF.33.0290	LmjF.33.0295	h-t	3.288
34	LmjF.34.0690	LmjF.34.0700	dss	3.402	LmjF.34.1240	LmjF.34.1245	h-t	1.428
					LmjF.34.2530	Lmj.34.2540	dss	6.258
					LmjF.34.3520	LmjF.34.3530	h-t	1.515
35	LmjF.35.1190	LmjF.35.1200	h-t	4.675	LmjF.35.0180	LmjF.35.0190	dss	2.323
					LmjF.35.1750	LmjF.35.1755	dss	3.028
					LmjF.35.1470	LmjF.35.1480	css	6.276
					LmjF.35.2590	LmjF.35.2600	css	0.814
					LmjF.35.2130	LmjF.35.2140	h-t	4.043
					LmjF.35.3470	LmjF.35.3480	h-t	3.373
					LmjF.35.3910	LmjF.35.3920	dss	1.508

Table 7-2. *(continue).*

	Origins				Non-origins			
Chr	Gene left	Gene right	SSR type	origin (kb)	Gene left	Gene right	SSR type	non-origin
36	LmjF.36.2720	LmjF.36.2730	h-t	6.401	LmjF.36.0535	LmjF.35.0537	dss	1.089
					LmjF.36.1955	LmjF.36.1960	dss	1.073
					LmjF.36.3660	LmjF.36.3670	dss	0.823
					LmjF.36.4220	LmjF.36.4230	h-t	1.037
					LmjF.36.5365	LmjF.36.5370	h-t	3.97
					LmjF.36.6350	LmjF.36.6360	h-t	2.112
					LmjF.36.1350	LmjF.36.1360	css	6.289
					LmjF.36.4880	LmjF.36.4890	css	1.442

Table 7-3. *L. mexicana* distance in Kbp between the first two genes within the SSRs, with or no origin activity detected by MFA-seq.

	Origins				Non-origins			
Chr	Gene left	Gene right	Type	origin (kb)	Gene left	Gene right	Type	non-origin
1	unclear				LmxM.01.0315	LmxM.01.0320	dss	0.969
2	LmxM.02.0570	LmxM.02.0580	dss	9.91	unclear			
3	LmxM.03.0670	LmxM.03.0690	css	12.691	LmxM.03.0010	LmxM.03.0020	dss	1.388
					LmxM.03.0970	LmxM.03.0980	h-t	0.703
4	LmxM.04.0380	LmxM.04.0390	css	8.378	LmxM.04.0625	LmxM.04.0630	h-t	0.706
5	LmxM.05.1040	LmxM.05.1050	dss	1.461	LmxM.05.0450	LmxM.05.0460	h-t	0.897
6	LmxM.06.0360	LmxM.06.0370	dss	4.647	LmxM.06.0560	LmxM.06.0570	h-t	1.385
					LmxM.06.1250	LmxM.06.1250	css	2.537
					the dss does not exist in L mex chr6			
7	LmxM.07.0470	LmxM.07.0475	dss	5.695	LmxM.07.0010	LmxM.07.0020	dss	5.033
					LmxM.07.0802	LmxM.07.0805	h-t	0.981
8	LmxM.08.1090	LmxM.08.1091	dss	11.346	LmxM.08.0860	LmxM.08.0870	css	3.343
9	LmxM.09.0690	LmxM.09.0700	css	6.591	LmxM.09.1000	LmxM.09.1010	dss	3.66
10	LmxM.10.0600	LmxM.10.6010	h-t	5.629	LmxM.10.1227	LmxM.10.1228	dss	1.178
					LmxM.10.0030	LmxM.10.0040	dss	9.675
					LmxM.10.0510	LmxM.10.0520	css	3.857
11	LmxM.11.0475	LmxM.11.0480	h-t	8.557	LmxM.11.0920	LmxM.11.0930	h-t	3.127
12	LmxM.12.0510	LmxM12.0520	dss	8.776	LmxM.12.0400	LmxM.12.0405	css	2.878
					LmxM.12.0010	LmxM.12.0020	h-t	0.399
13	LmxM.13.0450	LmxM.13.0460	dss	5.072	LmxM.13.0700	LmxM.13.0710	css	1.265
					LmxM.13.1370	LmxM.13.1380	h-t	1.012
					LmxM.13.1680	LmxM.13.1690	dss	1.833
14	LmxM.14.0470	LmxM.14.0480	css	8.147	LmxM.14.1050	LmxM.14.1060	dss	2.212
15	LmxM.15.0740	LmxM.15.0750	css	6.619	LmxM.15.0223	LmxM.15.0225	dss	1.049
					LmxM.15.1560	LmxM.15.1570	dss	4.47
16	LmxM.16.0920	LmxM.16.0930	dss	4.634	LmxM.16.1130	LmxM.16.1140	css	0.954
					LmxM.16.1520	LmxM.16.1530	dss	2.869
17	LmxM.17.0733	LmxM.17.0790	h-t	5.666	LmxM.17.0860	LmxM.17.0870	dss	1.59
					LmxM.17.0340	LmxM.17.0350	h-t	2.048
18	LmxM.18.1050	LmxM.18.1060	h-t	4.814	LmxM.18.0560	LmxM.18.0570	dss	1.904
19	LmxM.19.1420	LmxM.19.1430	h-t	6.663	LmxM.19.0980	LmxM.19.0985	h-t	5.007
					LmxM.19.0220	LmxM.19.0230	dss	7.342
20	LmxM.20.1175	LmxM.20.1180	h-t	6.661	LmxM.20.0840	LmxM.20.0850	h-t	0.694
					LmxM.20.0260	LmxM.20.0625	dss	1.313
					LmxM.20.1450	LmxM.20.1460	css	1.467
21	LmxM.21.0720	LxmM.21.0725	dss	6.302	LmxM.21.0015	LmxM.21.0020	dss	1.043
					LmxM.21.0520	LmxM.21.0530	css	1.765
					LmxM.21.1090	LmxM.21.1100	css	1.727
					LmxM.21.1720	LmxM.21.1730	dss	1.609

Table 7-3. *(continue).*

	Origins				Non-origins			
Chr	Gene left	Gene right	Type	origin (kb)	Gene left	Gene right	Type	non-origin
22	LmxM.22.1480	LmxM.22.1490	dss	5.98	LmxM.22.0790	LmxM.22.0800	dss	2.112
					LmxM.22.1220	LmxM.22.1230	css	0.842
					LmxM.22.0010	LmxM.22.0020	h-t	5.832
23	LmxM.23.1155	LmxM.23.1160	dss	4.65	LmxM.23.1630	LmxM.23.1640	css	3.121
					LmxM.23.0010	LmxM.23.0020	h-t	1.611
24	LmxM.24.1300	LmxM.24.1310	h-t	4.157	LmxM.24.0650	LmxM.24.0660	h-t	0.938
					LmxM.24.1900	LmxM.24.1905	h-t	0.507
					LmxM.24.2330	LmxM.24.2340	dss	1.225
					LmxM.24.1640	LmxM.24.1650	css	4.23
					LmxM.24.0010	LmxM.24.0020	h-t	0.678
25	LmxM.25.1460	LmxM.25.1470	h-t	1.202	LmxM.25.0715	LmxM.25.0720	dss	2.517
					LmxM.25.1080	LmxM.25.1090	css	2.333
					LmxM.25.2160	LmxM.25.2170	dss	1.357
26	LmxM.26.1665	LmxM.26.1670	h-t	5.612	LmxM.26.1015	LmxM.26.1020	dss	1.464
					LmxM.26.0760	LmxM.26.0770	h-t	0.802
					LmxM.26.2270	LmxM.26.2280	h-t	1.836
27	LmxM.27.2337	LmxM.27:rRNA:rfam scan:982402-983034	dss	14.154	LmxM.27.1265	LmxM.27.1270	dss	1.77
					LmxM.27.0290	LmxM.27.0300	dss	3.648
28	LmxM.28.2100	LmxM.28.2110	dss	3.946	LmxM.28.0770	LmxM.28.0785	dss	1.097
					LmxM.28.0350	LmxM.28.0360	css	0.701
					LmxM.28.1570	LmxM.28.1580	css	8.415
					LmxM.28.2690	LmxM.28.2700	css	0.758
8	-	-	-	-	LmxM.08_29.0890	LmxM.08_29.0885	dss	3.628
					LmxM.08_29.1810	LmxM.08_29.1800	h-t	2.495
					LmxM.08_29.1440	LmxM.08_29.1450	css	5.352
					LmxM.08_29.2360	LmxM.08_29.2350	dss	1.495
29	LmxM.29.0710	LmxM.29.0720	dss	3.719	LmxM.29.1730	LmxM.29.1740	h-t	0.865
					LmxM.29.2090	LmxM.29.2100	css	0.925
					LmxM.29.3235	LmxM.29.3240	dss	3.836
30	LmxM.30.1640	LmxM.30.1650	h-t	4.103	LmxM.30.0570	LmxM.30.0571	h-t	5.047
					LmxM.30.1230	LmxM.30.1240	h-t	2.952
					LmxM.30.1990	LmxM.30.2000	h-t	6.7
					LmxM.30.2715	LmxM.30.2720	h-t	0.991
					LmxM.30.3160	LmxM.30.3170	dss	1.681
31	LmxM.31.2985	LmxM.31.2990	dss	6.307	LmxM.31.2155	LmxM.31.2160	h-t	1.435
					LmxM.31.1370	LmxM.31.1380	css	3.042
					LmxM.31.0480	LmxM.31.0490	dss	1.899
32	LmxM.32.1610	LmxM.32.1620	h-t	5.452	LmxM.32.1790	LmxM.32.1800	dss	1.143
					LmxM.32.0600	LmxM.32.0605	dss	2.807
					LmxM.32.0290	LmxM.32.0295	h-t	3.939
33	LmxM.33.0690	LmxM.33.0700	dss	3.464	LmxM.33.1240	LmxM.33.1245	h-t	1.427
					LmxM.33.2530	LmxM.33.2540	dss	6.211
					LmxM.33.3520	LmxM.33.3530	h-t	1.668
34	LmxM.34.1190	LmxM.34.1200	h-t	3.981	LmxM.34.0180	LmxM.34.0190	dss	2.426
					LmxM.34.1750	LmxM.34.1755	dss	2.936
					LmxM.34.1470	LmxM.34.1480	css	5.334
					LmxM.34.2590	LmxM.34.2610	css	1.003
					LmxM.34.2130	LmxM.34.2140	h-t	4.037
					LmxM.34.3470	LmxM.34.3480	h-t	3.148
					LmxM.34.3910	LmxM.34.3920	dss	1.547

Table 7-3. *(continue).*

	Origins				Non-origins			
Chr	Gene left	Gene right	Type	origin (kb)	Gene left	Gene right	Type	non-origin
20	-	-	-	-	LmxM.36.2720	LmxM.36.2730	h-t	3.549
					LmxM.36.0535	LmxM.35.0537	dss	1.101
					LmxM.36.1955	LmxM.36.1960	dss	1.079
					LmxM.36.3660	LmxM.36.3670	dss	0.662
					LmxM.36.4220	LmxM.36.4230	h-t	1.089
					LmxM.36.5365	LmxM.36.5370	h-t	3.122
					LmxM.36.6350	LmxM.36.6360	h-t	2.098
					LmxM.36.1350	LmxM.36.1360	css	5.217
					LmxM.36.4870	LmxM.36.4890	css	1.394

List of References

Archer, S. K., Inchaustegui, D., Queiroz, R. & Clayton, C. (2011). The cell cycle regulated transcriptome of *Trypanosoma brucei*. *PLoS One,* **6**, e18425.

Godoy, P. D., Nogueira-Junior, L. A., Paes, L. S., Cornejo, A., Martins, R. M., Silber, A. M., Schenkman, S. & Elias, M. C. (2009). Trypanosome prereplication machinery contains a single functional orc1/cdc6 protein, which is typical of archaea. *Eukaryot Cell,* **8**, 1592-603.

Tiengwe, C., Marcello, L., Farr, H., Dickens, N., Kelly, S., Swiderski, M., Vaughan, D., Gull, K., Barry, J. D., Bell, S. D. & McCulloch, R. (2012). Genome-wide analysis reveals extensive functional interaction between DNA replication initiation and transcription in the genome of *Trypanosoma brucei*. *Cell Rep,* **2**, 185-97.